remote sensing

MDPI

Article

Multi-Temporal Remote Sensing for Forest Conservation and Management: A Case Study of the Gran Chaco in Central Argentina

Francisco G. Alaggia [1], Michele Innangi [2,*], Laura Cavallero [1,3], Dardo Rubén López [1,3], Federica Pontieri [2], Flavio Marzialetti [4,5], Ramon Riera-Tatché [2,6], Paolo Gamba [6] and Maria Laura Carranza [2,4]

1 Instituto Nacional de Tecnología Agropecuaria, Estación Forestal Villa Dolores (EEA Manfredi), Las Encrucijadas, Camino Viejo a San José, Km 1 Villa Dolores, Córdoba 5870, Argentina; franciscoalaggia@gmail.com (F.G.A.); cavallero.lauri@gmail.com (L.C.); lopez.dardor@inta.gob.ar (D.R.L.)
2 EnviXLab, Department of Biosciences and Territory, University of Molise, Contrada Fonte Lappone, 86090 Pesche, Italy; f.pontieri@studenti.unimol.it (F.P.); rrierat@gmail.com (R.R.-T.); carranza@unimol.it (M.L.C.)
3 Consejo Nacional de Investigaciones Científicas y Técnicas (CONICET), CCT Córdoba, Av. Ciudad de Valparaíso S/N, Córdoba 5000, Argentina
4 National Biodiversity Future Center (NBFC), 90133 Palermo, Italy; fmarzialetti@uniss.it
5 Department of Agricultural Sciences, University of Sassari, Viale Italia 39/a, 07100 Sassari, Italy
6 Department of Electrical, Biomedical and Computer Engineering, University of Pavia, Via Ferrata 5, 27100 Pavia, Italy; paolo.gamba@unipv.it
* Correspondence: michele.innangi@unimol.it

Abstract: Anthropogenic alteration of tropical and subtropical forests is a major driver of biodiversity loss; notably, the Chaco Forest, which is the largest dry forest in the Americas, is among the most impacted regions. Sustainable forest management, a key objective of the UN's 15th Sustainable Development Goal (SDG), underscores the need for advanced monitoring tools. This study integrates Sentinel-2 remote sensing (RS) spectral indices with field data to analyze forests under varying management regimes and levels of alteration in a representative area of the Chaco region (Chancaní Provincial Reserve and surrounding areas of the West Arid Chaco). Forest structure types and conservation levels were linked to monthly spectral index behavior using linear mixed models. Spectral indices such as the BI (Brightness Index), $NDWI_{Gao}$ (Normalized Difference Water Index), and $MCARI_{Sent}$ (Modified Chlorophyll Absorption in Reflectance Index) effectively differentiated forest stands by conservation status and structural alteration. This combined RS and field data approach proved highly effective for detecting and characterizing forests with diverse conservation and sustainability conditions. The methodology demonstrates significant potential as a reliable RS-based tool for monitoring forest health and supporting progress toward SDG targets, particularly in regions like the Chaco Forest, which face extensive anthropogenic pressures.

Keywords: ecosystem monitoring; structural alteration index; RS indexes phenology; Sentinel-2

Academic Editor: Hubert Hasenauer

Received: 20 December 2024
Revised: 7 February 2025
Accepted: 19 February 2025
Published: 21 February 2025

Citation: Alaggia, F.G.; Innangi, M.; Cavallero, L.; López, D.R.; Pontieri, F.; Marzialetti, F.; Riera-Tatché, R.; Gamba, P.; Carranza, M.L. Multi-Temporal Remote Sensing for Forest Conservation and Management: A Case Study of the Gran Chaco in Central Argentina. *Remote Sens.* **2025**, *17*, 748. https://doi.org/10.3390/rs17050748

1. Introduction

Forest ecosystems have played a major role in human history, and forest management has accompanied population growth and development worldwide for thousands of years [1]. The extent of anthropogenic alteration and degradation of natural forests in many tropical and subtropical ecosystems is one of the main causes of biodiversity

loss worldwide [2,3]. Forest degradation is a process that diminishes the biodiversity and functioning of these ecosystems [4]. Rather than reducing forest area, degradation involves the deterioration of the structure and composition of woody plant biomass, leading to a decline in the forest's overall quality [4]. Thus, degradation directly results in a long-term loss of the forest's capacity for carbon storage [5] and its ability to provide goods and services [6].

Identifying effective strategies for forest management is a crucial challenge of the Anthropocene Epoch. In response to this challenge, the United Nations included forest management and governance strategies in the 2030 Sustainable Development Agenda (SDG) [7]. The 15th SDG states, "Protect, restore and promote sustainable use of terrestrial ecosystems, sustainably manage forests, combat desertification, and halt and reverse land degradation and halt biodiversity loss". Achieving this goal requires significant efforts to develop effective monitoring tools that illustrate sustainable management practices and support policymakers [1].

In this context, remote sensing (RS) could provide valuable support as an effective source of data and methods for forest monitoring, offering a cost-effective option for frequent observation of large areas [8]. RS provides multi-temporal data at various spatial scales in a cost-effective, spatially contiguous, and timely manner, supporting standardized assessments of forest cover and fragmentation [1,9]. However, while RS is particularly effective for producing forest cover maps with explicit information on forest distribution, using RS to quantify forest degradation is more challenging. In such cases, the area remains forested but undergoes structural, compositional, and functional alterations [10]. Recent advancements in satellite imaging, algorithms, and computing now enable high-resolution, large-scale mapping of forest disturbances [8]. While most studies focus on boreal, temperate, and tropical wet forests, the mapping of forest alterations in subtropical semi-arid regions has only recently gained attention [11,12]. To accurately assess forest characteristics in bio-climatic regions with strong seasonality, RS techniques can be combined with approaches that capture spatial and temporal vegetation patterns [13]. For instance, analyzing ecosystem phenological properties, which are driven by climatic seasonality [14], is an effective method for mapping intense seasonal biomass variations, such as those that characterize subtropical forests [15,16].

The implementation of RS for mapping forest characteristics worldwide, particularly in subtropical and developing countries where natural forests face significant pressure, greatly benefits from the availability of free satellite imagery with good spatial resolution and high revisit frequency, such as that provided by the SENTINEL satellite constellation [8,16]. These studies primarily rely on remote sensing data, as further research is needed to integrate remote sensing with conservation and alteration metrics obtained through field measurements [17,18].

The Gran Chaco, one of the largest seasonally dry subtropical forests in the world, spans Argentina, Paraguay, Brazil, and Bolivia [19,20]. It is also one of the most threatened ecosystems in Latin America [3]. Forest fragmentation and degradation, driven by unsustainable practices such as logging, firewood collection, charcoal production, and livestock grazing [9,21–24], have significantly impacted the Chaco Forest. Numerous studies have documented how the overuse of Chaco forests leads to biodiversity loss [25–30], changes in surface and groundwater hydrological cycles [31–36], and soil loss, which contributes to the advancement of land desertification [33,35]. Furthermore, forest degradation leads to increased carbon dioxide emissions into the atmosphere [36–39].

Previous studies in the Chaco region have examined the effects of anthropogenic and natural disturbances on plant community phenology using RS data [11,40,41]. Most of these studies have focused on the Normalized Difference Vegetation Index (NDVI),

widely recognized for its ability to assess the fraction of photosynthetically active radiation absorbed by vegetation [42–44]. Recently, however, advancements in satellite data and processing power have enabled the exploration of additional spectral indices with enhanced spatial and temporal resolution and faster processing speeds [18,45]. These new tools provide opportunities for detailed phenological analyses and the development of novel indicators for sustainable management specifically tailored to the Chaco region.

This study aims to explore the potential of spectral indices derived from Sentinel-2 remote sensing data, combined with field data, as indicators of forest structural integrity and degradation resulting from sustainable or unsustainable management practices in the Arid Chaco forests. We hypothesize that the phenological patterns of RS ecological indices vary depending on forest characteristics and the degree of alteration. To test this hypothesis, we calculated a series of spectral indices useful for RS-based ecosystem descriptions, including those related to photosynthetic activity and biomass, canopy water content and moisture, water stress, soil characteristics, chlorophyll and carotenoid content, and fire-induced stress.

We then performed a Variance Inflation Factor (VIF) analysis to identify and retain only the variables with low multicollinearity, ensuring a focus on minimally correlated variables. Next, we assessed the relationship between this set of low-correlated spectral indices and field-collected data on forest structures across ecosystems with varying levels of structural alteration. Specifically, based on a set of minimally correlated monthly RS spectral variables and field data, we addressed the following questions:

(a) Do forests with different management regimes, levels of degradation (structural alteration), and dominant species exhibit different spectral phenology (i.e., the study of seasonal changes in vegetation as observed through spectral indices)?
(b) Which indices effectively differentiate forests with different levels of structural degradation?

Validating our hypothesis—that in highly seasonal subtropical forests, the phenological patterns of remote sensing (RS) ecological indices vary with ecosystem characteristics and the degree of alteration—could provide further evidence of RS as a powerful proxy for modeling forest attributes. The integration of a statistically adequate number of field samples with monthly Sentinel RS ecological indices would strengthen our ability to conduct accurate, large-scale assessments at a significantly lower cost than relying solely on traditional field inventories.

2. Materials and Methods

2.1. Study Area

The study area is located in the southern sector of the dry Chaco in central Argentina (Figure 1) and is representative of the Chaco Phytogeographical Province [20]. It includes a protected area (Chancaní Provincial Reserve) and surrounding forests with different management regimes and levels of degradation (Figure 1A). Although these forests provide essential ecosystem services to local communities and contribute to the regional economy [46,47], making them valuable for conservation and sustainable management, the region's permissive and liberal legal regulations fail to prevent deforestation and degradation [48].

The study area comprises two main geomorphological landscapes: foothills and plains (Figure 1B). The foothills, located on the western slopes of the Sierras de Pocho, range from 370 to 500 m above sea level and have permeable, poorly developed soils. The plains, the most extensive landform, feature gentle slopes of less than 1% and sedimentary deposits with sandy or clayey soils of low fertility, which are prone to erosion [49,50]. The region has a subtropical xeric climate [51], characterized by a dry season, high evapotranspiration [33],

and a mean annual rainfall of 600 mm, mostly occurring between October and April. The average annual temperature is 18 °C [52].

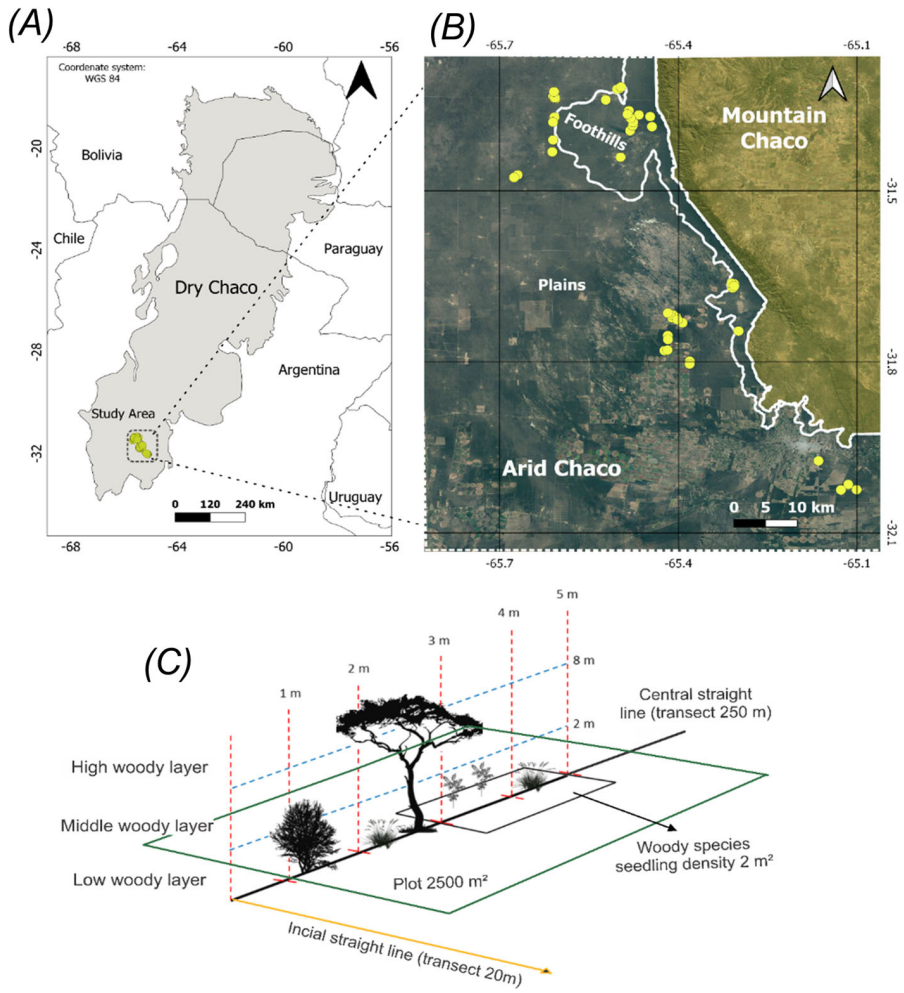

Figure 1. (**A**) Location of the study area (dotted-line box) within the dry Chaco (gray area). (**B**) Distribution of sampling sites (yellow circles) used for field data collection and Sentinel-2A image analysis across foothills and plains within the Arid Chaco landscape. (**C**) Methodological scheme illustrating field data collection through plot-based surveys and sampling transects. Maps have been prepared on QGIS Development Team (2024). QGIS Geographic Information System (Version 3.34). Open Source Geospatial Foundation Project. Maps Data: Google, ©2024 Airbus.

The vegetation of the study area includes xerophilous subtropical forests [19] and shrublands [51,53]. In the foothills, forests are dominated by *Aspidosperma quebracho-blanco* Schltdl., accompanied by isolated individuals of *Neltuma flexuosa* (DC.) C. E. Hughes and G. P. Lewis, *Sarcomphalus mistol* (Griseb.) Hauenschild, *Neltuma torquata* (Lag.) DC., *Neltuma chilensis* (Molina) C. E. Hughes and G. P. Lewis, and *Celtis iguanaea* (Jacq.) Sarg. The tree layer can reach heights of up to 15 m and is dominated by *A. quebracho-blanco*, while the shrubby layer, reaching heights of up to 4 m, is primarily composed of *Larrea divaricata* Cav., *Mimozyganthus carinatus* (Griseb.) Burkart, *Senegalia gilliesii* (Steud.) Seigler and Ebinger, and *Celtis pallida* Torr.

In the western plains, forests are co-dominated by *A. quebracho-blanco* and *N. flexuosa*, with shrub cover exceeding 60%, depending on the level of biodiversity conservation. The dominant shrub species in these areas include *L. divaricata*, *M. carinatus*, *S. gilliesii*, and *C. pallida*. In the southern and central depressed areas, which have higher moisture levels and finer soils, plant communities are dominated by *N. flexuosa* and *C. pallida*. In the northern

saline lowlands, plant communities are dominated by halophilic species such as *Geoffroea decorticans* (Gillies ex Hook. and Arn.) Burkart, *Allenrolfea* spp. Kuntze, *Suaeda* spp., and *Atriplex cordobensis* Gand. and Stuck [50,54–56].

Shrub communities vary in composition and height. Mixed shrublands often exhibit two layers (shrubby and herbaceous) with some isolated trees under 5 m tall (*A. quebracho-blanco* and *N. flexuosa*). The shrubby layer is usually dominated by *L. divaricata*, *M. carinatus*, and *S. gilliesii*. In significantly degraded areas, the proportion of bare soil is high, while woody species diversity is low. In some locations, woody communities have been replaced by sprayed crops such as potatoes, corn, and wheat or by implanted *Cenchrus ciliaris* L. (buffel grass) pastures with scattered small trees [57].

2.2. Definition and Selection of Sampling Sites

Field data were collected between 2017 and 2019 from 49 sampling sites across a 300,000-hectare area in the southeastern sector of the Arid Chaco, encompassing both major landscapes: plains and foothills (Figure 1). Sampling was conducted using a stratified approach, incorporating Google Earth Pro (Google LLC, Mountain View, CA, USA; version 7.3.7) and expert knowledge, along a gradient of land use history and conservation levels. The conservation level was classified on a scale from 1 (very high) to 8 (very low), based on the extent of structural and species composition modifications within the natural ecosystem matrix. Logistical factors, such as accessibility via roads or trails and obtaining permits from public and private landowners, also influenced site selection. The sampling strategy was designed to comprehensively capture the area's heterogeneity by considering geomorphological landscapes, vegetation types, management practices, and levels of structural degradation.

Following previous studies in the forests of the Arid Chaco and other regions [57], we defined a sample size that was statistically robust and representative [58], while ensuring that the fieldwork effort remained manageable within a limited time frame and with the available staff (see [50] for details).

A minimum distance of 1 km was maintained between sampling sites. Within each landscape (foothills and plains), we selected mature, well-preserved forests that had remained undisturbed for at least the past 30 years (e.g., mature forests without signs of grazing, browsing, or logging, and without evident soil erosion) to serve as reference sites. These reference forests included Chancaní Forest Reserve (representative of the foothill landscape; 31°21′22″ S, 65°27′29″ W) and a forest relic located on a private property, *Estancia El Álamo* (representative of the plain landscape; 31°43′28.54″ S, 65°24′11.78″ W).

Additional sampling sites were selected in the surroundings of the reference sites, maintaining similar soil types, topography, and potential plant communities (e.g., same ecological site *sensu* [59]) but differing in management practices, resulting in distinct physiognomies. These included closed forests with emergent trees, closed forests without emergent trees, low closed forests, open forests, natural grasslands, and cultivated pastures (Table 1).

Table 1. Forest classes sampled in the study area including common name, landscape type, land-use management history, number of sampling sites, and the conservation level (CL: with higher conservation values close to 1 and lower than 8).

Forest Class/ Structure-Physiognomy	Landscape	Land Use History	N° Sites	CL
Mature forest of *Neltuma flexuosa* and/or *Aspidosperma quebracho blanco*. Common name: Mature forests on foothills	Foothills	Natural protected areas with limited logging or livestock grazing for at least five decades.	7	1
Mature forest of *Neltuma flexuosa* and/or *Aspidosperma quebracho blanco*. Common name: Mature forests on plains	Plains	Scarce logging or livestock grazing for at least five decades.	2	2

Table 1. *Cont.*

Forest Class/ Structure-Physiognomy	Landscape	Land Use History	N° Sites	CL
Closed forest with emergent trees of *Neltuma flexuosa* and/or *Aspidosperma quebracho blanco*, with understory dominated by *Mimozyganthus carinatus*. Common name: Closed forests on foothills	Foothills	Low to moderate livestock forestry pressure. Selective felling of large (e.g., >40 cm diameter at breast height), with intervals of more than 20 years. Annual stocking rate lower ** than 1 * Cow Equivalent (CE)/20 hectares, grazing in autumn–winter. Seasonal supplement, small plots (e.g., <3% of the farm area) with megathermal pastures.	6	3
Closed forest with emergent trees of *Neltuma flexuosa* and/or *Aspidosperma quebracho blanco*, with understory dominated by *Mimozyganthus carinatus*. Common name: Closed forests on plains	Plains	Low to moderate livestock forestry pressure. Selective felling of large trees (e.g., >40 cm diameter at breast height), with intervals of more than 20 years. Annual stocking rate lower ** than 1 * CE/20 ha., grazing in autumn–winter. Seasonal supplement, small plots (e.g., <3% of the farm area) with megathermal.	4	4
Closed forest of *Neltuma flexuosa*, *Larrea divaricata*, *Mimozyganthus carinatus*, and/or *Parkinsonia praecox*. Common name: Low closed forest	Foothills and plains	No mature trees remained, no resting periods or forest management. Low logging for firewood extraction. Stocking rate moderate to high (e.g., 1 CE/5 ha). Some time with fires.	10	5
Low closed forest of *Neltuma flexuosa*, *Aspidosperma quebracho blanco*, *Larrea divaricata*, *Mimozyganthus carinatus*, and/or *Celtis ehrenbergiana*. Common name: Shrublands	Foothills and plains	Fires or total logging of trees have occurred, followed by a high post-fire stoking rate. Moderate to heavy logging, moderate to high stocking rate of cows and/or goats (e.g., more than 1 CE/2–4 ha, sustained for more than a decade).	10	6
Open forest of *Neltuma flexuosa*, *Mimozyganthus carinatus*, and/or *Celtis ehrenbergiana*. Common name: Savannas	Foothills and plains	Heavy logging and high stocking rate of cows and/or goats over the past decades, with mechanical shrub removal and/or partial felling of the woody layer every 3 to 5 years (e.g., 50 to 70% of shrub cover is removed). Carrying capacity is declining due to reduced productivity caused by chronic degradation.	6	7
Natural grassland and implanted pastures with *Tricloris* sp. and/or *Cencrus ciliaris*. Isolated individuals of *Neltuma flexuosa* and *Aspidosperma quebracho blanco*. Common name: Grasslands with trees	Foothills and plains	Sites cleared totally or partially for grassland productivity and/or to establish megathermal grass pastures. High livestock density with significant anthropic input (e.g., rolling every 3 to 5 years with interplanting, removing more than 80% of woody cover). Livestock stocking rate 1 CE/ha.	4	8
TOTAL			49	

* Cow Equivalent (CE) is the annual average requirements of a 400 kg cow, which gestates and raises a calf until weaning at 6 months of age, weighing 160 kg, including the forage consumed by the calf. ** Low annual stocking rate means that forage production is greater than livestock forage consumption. Moderate annual stocking rate implies that forage production is similar to livestock forage consumption. High annual stocking rate means that livestock forage consumption is greater than ecosystem forage production (i.e., exceeds carrying capacity).

2.3. Remote Sensing Data

For RS data, we utilized a monthly time series of freely available Sentinel-2 (S2) images, ensuring the closest possible alignment with the field data collection period (2020). Sentinel-2 imagery (European Space Agency, ESA, Paris, France) was obtained from the Copernicus Data Space repository (https://browser.dataspace.copernicus.eu, accessed on 14 December 2024). The Sentinel-2 constellation, comprising Sentinel-2A (S2A) and Sentinel-2B (S2B), is equipped with a multispectral instrument (MSI) that captures data in 13 spectral bands across the visible, near-infrared, and shortwave infrared regions of the electromagnetic spectrum. Sentinel-2 satellites provide high and medium spatial resolutions (10 m, 20 m, and 60 m) and have a high revisit frequency of five days at the equator [60].

Since the study area spans two Sentinel-2 grid tiles (T20JKL, T20HKK), we downloaded monthly S2 images for each tile (12 images per tile, totaling 24 images) at processing level 2A (Bottom-Of-Atmosphere, BOA). These images are geometrically orthorectified, co-registered, and atmospherically corrected to surface reflectance by ESA using the Sen2cor processor (version 2.11.0, European Space Agency, Paris, France) [61]. This processor applies atmospheric correction, terrain and cirrus correction, and scene classification to Sentinel-2 Level 1C (Top-Of-Atmosphere, TOA) imagery [61].

Only S2 images with low cloud coverage (<10%) were selected (S1, Table S1.1), and none of the 49 forest sample sites were affected by cloud cover in any month. All selected images were acquired at the same time (14:16–14:17), with sun zenith angles ranging from 24.361° to 61.536°. The Sen2cor processor applies bilinear interpolation using Lambert's reflectance law to minimize errors caused by shadows affecting spectral responses (S1, Table S1.1) [61]. Temporal alignment between RS and field data was ensured, as the measured variables remain stable over short periods in the Arid Chaco [62]. These variables typically do not change significantly within a few years unless extreme events such as wildfires or deforestation occur, none of which were recorded during the study period.

We used a subset of Sentinel-2 bands to calculate spectral indices, including bands at 10 m spatial resolution (e.g., blue: 490 nm, green: 560 nm, red: 665 nm, and near-infrared [NIR]: 842 nm) and bands at 20 m spatial resolution (e.g., red edge [RE]: 705 nm, Shortwave Infrared [SWIR]: 1610 nm and 2190 nm). All bands were resampled to a 20 m spatial resolution using the nearest neighbor method.

2.4. Field Data

At each sampling site (Figure 1C), a 2500 m^2 plot (250 m × 10 m) was established to collect ecological variables relevant to forest composition and disturbance analysis [17,58]. A central straight-line transect of 250 m intersected the plot, with an additional perpendicular transect of 20 m placed at the beginning of the plot [63].

Vegetation and bare soil cover were recorded using the point-intercept method [64] at 1-m intervals along the 250-m transect [63,64]. The ratio of vegetation cover to bare soil is a key indicator of Chaco vegetation integrity, where mature forests exhibit high vegetation cover, while disturbed areas are characterized by an increase in bare soil [20,49].

Additionally, we recorded vegetation structure parameters related to forest composition and degradation [17,50]. Vertical space was divided into four layers: one herbaceous layer and three woody layers (low < 2 m, medium 2–8 m, and high > 8 m). Every 5 m, we measured the maximum height of species recorded in each vegetation layer and counted the number of seedlings (0–30 cm height) within a 2 m^2 subplot [58,63].

On the perpendicular 20-m transect, we collected a composite litter sample, consisting of 10 sub-samples (each 40 cm^2) taken every 2 m. Finally, within the 2500 m^2 plot (250 m × 10 m), we recorded tree species density (for individuals > 5 cm in diameter) and measured their diameter at breast height (DBH) (Table 2).

Table 2. Field sampling scheme and forest variables measured (adapted from [29,58,63]).

Field Sampling Scheme	Forest Variable
Central straight line (transect) 250 m	-Woody sp. cover (total; for each species and for each vegetation layer: low < 2 m, medium 2–8 m, and high >8 m) and the derived horizontal heterogeneity index. -Bare soil cover (m). -Maximum height of the woody species (m; measurement carried out every 5 m, and the derived vertical heterogeneity index.
Plot woody species seedling density (2 m^2; 50 plots along the 250 m transect).	-Woody species seedling density (seedlings*ha^{-1}).
Initial straight line (transect) 20 m	-Composite litter sample (comprising 10 sub-samples taken every 2 m).
Plot 2500 m^2	-Tree density (trees*ha^{-1}). -Basal area (m^2*ha^{-1}).

The structural and compositional variables of woody vegetation (e.g., cover and height by species, litter characteristics) are commonly used descriptors of the main vegetation types in the Chaco region [20,53], as well as for assessing their structural integrity and degree of alteration [17,29,58,65].

The structural and compositional variables measured during fieldwork (2017–2019), such as tree height, basal area, and woody species cover, remain relatively stable over short timescales in arid ecosystems like the Arid Chaco [62]. This stability ensures a reliable temporal alignment between the field data and the selected RS images from 2020. Moreover, these variables typically do not undergo significant changes within a single year, unless extreme events such as wildfires or severe deforestation occur—none of which were recorded during the study period.

2.5. Data Processing

RS Spectral Indices

For each month, we calculated a series of 22 spectral indices useful for remote sensing (RS)-based ecosystem descriptions (for the complete list of calculated indices (see S1, Table S1.2) within the 49 forest sample sites. The analyzed spectral indices serve as indicators of photosynthetic activity and biomass, canopy water content and moisture, water stress, soil characteristics, chlorophyll and carotenoid content, and fire-induced stress.

Since many spectral indices exhibit high correlation with one another, we conducted a Variance Inflation Factor (VIF) analysis to eliminate redundant variables, ensuring that the retained indices were statistically independent. Accordingly, we selected three RS variables with VIF values lower than 5 for further analysis [66]. These selected indices (Table 3) include the following: Modified Chlorophyll Absorption in Reflectance Index ($MCARI_{Sent}$)—an indicator of leaf chlorophyll content [67]; Normalized Difference Water Index ($NDWI_{Gao}$)—an indicator of leaf water content [68]; Brightness Index 2 (BI_2)—an indicator of surface presence and soil moisture [69].

The $MCARI_{Sent}$ index combines red edge, red, and green bands to estimate the depth of chlorophyll absorption (Table 3). It is highly sensitive to leaf chlorophyll content and strongly correlates with the Leaf Area Index. Additionally, $MCARI_{Sent}$ values are not affected by illumination conditions, soil background reflectance, or other non-photosynthetic materials [67].

The $NDWI_{Gao}$ index estimates leaf water content through a normalized difference of NIR and SWIR bands (Table 3). It is sensitive to changes in canopy water content and useful for estimating water stress levels. The typical $NDWI_{Gao}$ range for green vegetation is −0.1 to 0.4, with 0.4 indicating high leaf water content [68].

The BI_2 index is sensitive to soil brightness and quantifies bare surfaces by calculating the square root of brightness for each pixel (Table 3). It effectively differentiates bare soil from

vegetation in arid environments. The BI_2 index ranges from 0 (indicating no bare surfaces) to higher positive values, which correspond to increasing percentages of bare surfaces [69].

We focused on monthly data, as they are particularly effective for tracking fine-scale ecological temporal variations, which are especially pronounced in subtropical semiarid systems such as the Arid Chaco, where vegetation undergoes strong seasonal fluctuations. The high temporal resolution of our analysis captures phenological differences across forest types and management regimes, offering a detailed view of forest condition dynamics. This approach is well-suited to detecting intra-annual variations, which are essential for assessing forest degradation processes that do not follow a uniform yearly pattern.

Table 3. Spectral indices describing forest characteristics derived from Sentinel-2 imagery, retained for further analysis due to low multicollinearity (VIF < 5).

Acronym	Name	Formula	Proxy	Reference
$MCARI_{Sent}$	Modified Chlorophyll Absorption in Reflectance Index	$((RED\ EDGE - RED) - 0.2(RED\ EDGE - GREEN)) * RED\ EDGE/RED((RED\ EDGE - RED) - 0.2(RED\ EDGE - GREEN)) * RED\ EDGE/RED$	Leaf chlorophyll content	[67]
$NDWI_{Gao}$	Normalized Difference Water Index	$\frac{NIR-SWIR}{NIR+SWIR}\ \frac{NIR-SWIR}{NIR+SWIR}$	Leaf water content	[68]
BI_2	Brightness Index 2	$\sqrt{\frac{RED^2+GREEN^2+NIR^2}{3}}\sqrt{\frac{RED^2+GREEN^2+NIR^2}{3}}$	Presence of bare surfaces	[69]

2.6. Data Analysis

2.6.1. Phenological Analysis of RS Variables

We utilized linear mixed models (LMMs) to capture the spatial and temporal variations of spectral indices across the eight levels of forest conservation (Table 1). The LMM approach was chosen for its ability to explicitly handle both fixed and random effects, making it well-suited for addressing temporal heterogeneity across semi-arid seasonal ecosystems. Specifically, to account for spatio-temporal heterogeneity in LMMs, we included forest type as a fixed effect, as it represents the primary factor influencing spectral variation and conservation status, while transect ID and month were included as random effects, accounting for variability at different spatial locations and across time. The interaction term (Transect ID × Month) was introduced to account for site-specific seasonal patterns, ensuring that temporal changes were analyzed within each site rather than being treated as uniform across the study area. This allowed us to explicitly model seasonal variation at each site, ensuring that different forests could exhibit distinct temporal dynamics.

As for seasonal and geospatial differences, the random effect for Transect ID captures the inherent spatial variability among sampling sites, while the random effect for Month accounts for differences across time points, allowing us to model phenological changes in spectral indices. The inclusion of these random effects improves model transparency and prevents pseudo-replication, ensuring that repeated measurements from the same sites are not treated as independent observations. The denominator degrees of freedom were calculated using the Kenward–Roger approach. The intra-class correlation coefficient (ICC) was presented as an indicator of the extent of random variance in the models. The quality of fit for mixed models was assessed using conditional and marginal determination coefficients (R^2c and R^2m) to quantify unbiased assessments of variance explained by fixed effects alone and by fixed plus random effects, respectively [70].

After analyzing the models, we computed the marginal mean and the accompanying 95% confidence interval for each spectral index. We then conducted a Tukey test with Bonferroni correction to determine whether there were statistically significant differences between the forest classes. We used the R programming language (version 4.3.2 [71]) for all analyses, implementing the following packages: 'ggplot2' (version 3.5.1) [72] for data visualization, 'lme4' [73] for mixed-effects modeling, 'rstatix' (version 0.7.2) [74] for

statistical tests, 'multcomp' (version 1.4-28) [75] for multiple comparisons, 'sjPlot' (version 2.8.17) [76] for visualizing model outputs, and 'usdm' (version 2.1-7) [77] for addressing multicollinearity in ecological data.

2.6.2. Structural Alteration Index Across Forest Classes

Based on field data, we estimated the Structural Alteration Index (*SAI*) for each site (see [65,78] for details), a well-established proxy for ecosystem degradation previously tested in other forests in Argentina (e.g., [29,58]). The *SAI* is a multivariate index that summarizes the structural and compositional deviation of the sampled forest relative to a non-disturbed "reference" site, previously defined for the study area [65,78].

To maintain a balanced ratio between variables and the number of plots, we selected variables for *SAI* calculation in each environment (foothill or plain) using a multivariate approach. Specifically, we conducted a Principal Components Analysis (PCA) on site-by-structure-composition variable matrices, retaining those variables that contributed the most to data variability (e.g., explaining PCA1 and PCA2) to calculate *SAI* (see S2, Table S2.1; Figures S2.1 and S2.2).

The variables retained for *SAI* calculation included litter dry weight (ton·ha^{-1}), bare soil (%), Vertical Heterogeneity Index (VHI) [58], Horizontal Heterogeneity Index (HHI) [58,65], woody species seedling density (seedlings·ha^{-1}), tree density (trees·ha^{-1}), basal area (m^2·ha^{-1}), and cover percentages of key species: *G. decorticans*, *C. ehrenbergiana*, *P. praecox*, *N. flexuosa*, and *A. quebracho-blanco* in the low (0–2 m) and medium (2–8 m) vegetation layers, as well as *L. divaricata* cover in both layers (see S2, Table S2.1; Figures S2.2 and S2.4). These variables describe the most important ecological characteristics of Arid Chaco Forest ecosystems, including vegetation physiognomy, resilience, soil composition, and key woody species [20,49].

Based on multivariate matrices (sites × selected structure and composition variables), *SAI* values for each site were computed using the Mahalanobis Distance (MD) [79] from the reference forest community (e.g., well-preserved forest). Sample sizes were n = 30 for plains and n = 19 for foothills. The Mahalanobis Distance accounts for variable correlation and weights each variable by its variance, making it applicable across different scales and independent of measurement units [79]. The Structural Alteration Index (*SAI*) was calculated as follows:

$$SAI = \left[(MD_i \times 100) \times \left(MD_{max}\right)^{-1}\right] SAI = \left[(MD_i \times 100) \times \left(MD_{max}\right)^{-1}\right] \quad (1)$$

where MD_i is the Mahalanobis Distance between the i-th site and the reference site, and MD_{max} corresponds to the maximum registered *MD* value. Based on *MD*, *SAI* integrates structural and compositional variables, accounting for variable correlation and scaling differences. *SAI* captures both the deviation of degraded sites from reference conditions and the multidimensional nature of ecosystem alteration. The inclusion of physiognomic and species-specific variables indicative of degradation strengthens the ecological relevance of *SAI* in the context of the Arid Chaco Forest [78].

2.6.3. Exploring the Relationship Between RS Ecological Variables and Field-Measured *SAI* Values

We evaluated the relationship between the spectral indices and the Structural Alteration Index (*SAI*) using general linear models (GLMs). *SAI* was included as a predictor variable, while the average values (monthly and annual) of each spectral index (BI_2, $MCARI_{Sent}$, and $NDWI_{Gao}$) were included as response variables in the GLMs (13 GLMs per spectral index). The landscape (plains and foothills) was included as a categorical predictor. To assess the normality of residuals, we performed the Shapiro–Wilk normality test. Additionally, we calculated the Akaike Information Criterion (AIC) for each model

and compared it with the AIC of a null model [80]. The analyses were conducted in R version 4.3.2 [71] using the packages 'ggplot2' [72], 'sf' [81], and 'terra' [82].

3. Results

3.1. Phenological Behavior of RS Variables Across Forest Classes

Spectral indices varied significantly between forest types with different conservation statuses (Figure 2, Table 4). Two out of three models, except $MCARI_{Sent}$, showed a conditional R^2 higher than 0.9. In some cases, the impact of the random component on the model was significant, as observed for $MCARI_{Sent}$ and $NDWI_{Gao}$.

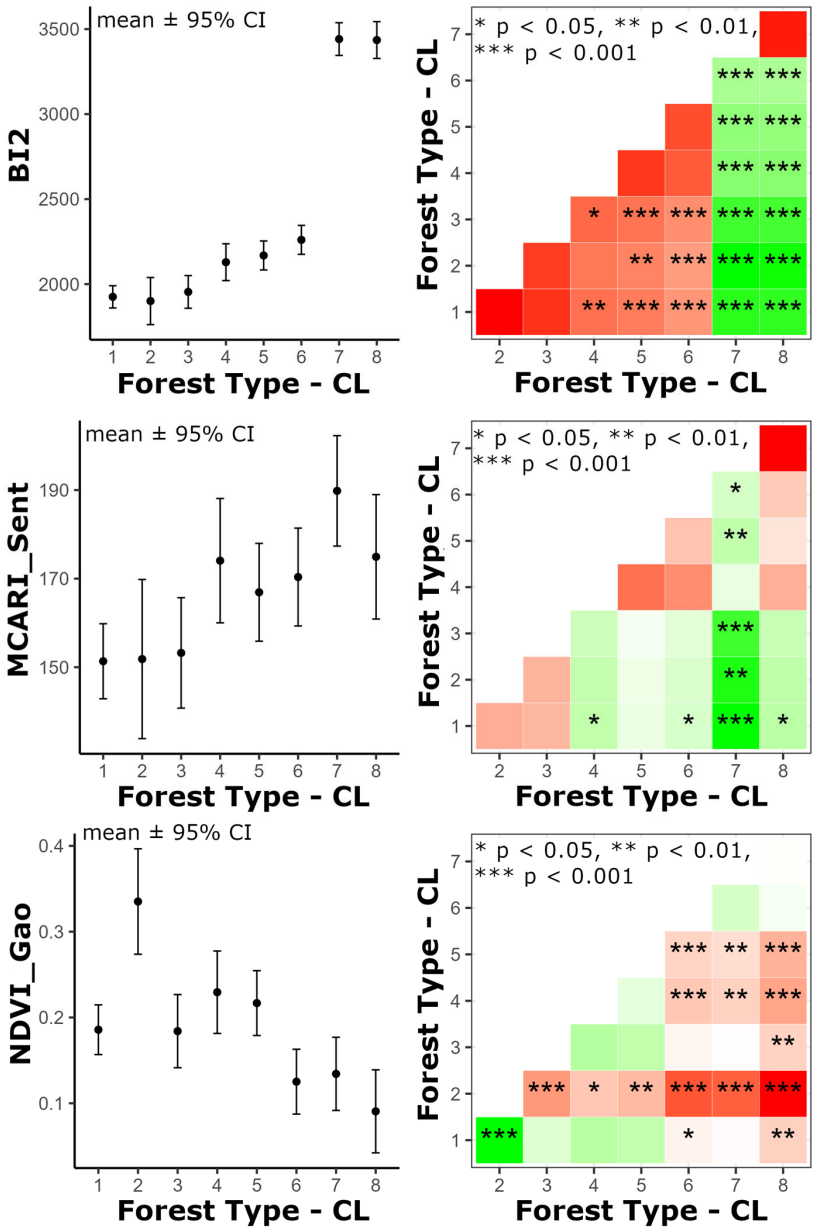

Figure 2. Marginal means of spectral indices for the eight forest types, estimated via a linear mixed model. The left panel shows mean values with 95% confidence intervals, while the right panel compares forest ecosystems. Green cells indicate higher average values for the column forest type; red cells indicate the opposite. Asterisks denote significance: * $p < 0.05$, ** $p < 0.01$, *** $p < 0.001$. Forest types and conservation levels (CL) are as follows: mature forests on foothills (CL 1), plains (CL 2); closed forests on foothills (CL 3), plains (CL 4), low closed forests (CL 5), shrublands (CL 6), savannas (CL 7), grasslands with trees (CL 8).

Table 4. Linear mixed models (LMMs) of spectral indices by forest conservation classes. The fixed component of the model provides estimates, confidence intervals (CIs), and *p*-values for both the intercept and slope. The random effects are presented as explained variance (σ2), variance of the random intercept (τ00), and intra-class correlation coefficient (ICC). The goodness-of-fit is quantified using marginal and conditional R^2 values, which respectively capture the impact of fixed and fixed + random components in the model. Forest types and conservation levels (CL number) refer to mature forests on foothills (CL 1), mature forests on plains (CL 2), closed forests on foothills (CL 3), closed forests on plains (CL 4), low closed forests (CL 5), shrublands (CL 6), savannas (CL 7), and grasslands with trees (CL 8).

		BI_2		$MCARI_{Sent}$		$NDWI_{Gao}$	
Predictors	**Estimates**	**CI**	**Estimates**	**CI**	**Estimates**	**CI**	
Interc.	1925.15 ***	1859.50–1990.80	151.35 ***	142.83–159.87	0.19 ***	0.16–0.21	
CL 2	−24.74	−163.98–114.51	0.49	−17.58–18.55	0.15 ***	0.09–0.21	
CL 3	29.02	−67.60–125.65	1.88	−10.66–14.42	−0.00	−0.04–0.04	
CL 4	203.88 ***	95.04–312.72	22.71 **	8.60–36.83	0.04	−0.00–0.09	
CL 5	243.49 ***	157.91–329.07	15.57 **	4.47–26.67	0.03	−0.01–0.07	
CL6	335.22 ***	249.63–420.81	19.02 ***	7.91–30.12	−0.06 **	−0.10–−0.02	
CL 7	1516.11 ***	1419.49–1612.74	38.47 ***	25.94–51.01	−0.05 *	−0.09–−0.01	
CL8	1510.42 ***	1401.56–1619.28	23.59 **	9.46–37.71	−0.10 ***	−0.14–−0.05	
			Random Effects				
σ^2		33,259.42		1316.25	0.00		
τ_{00}		93,595.66 $_{ID\_transect:Month}$		1561.27 $_{ID\_transect:Month}$	0.02 $_{ID\_transect:Month}$		
ICC		0.74		0.54	0.91		
N		49 $_{ID\_transect}$ 12 $_{Month}$		49 $_{ID\_transect}$ 12 $_{Month}$	49 $_{ID\_transect}$ 12 $_{Month}$		
Observ		33,157		33073	33120		
Marg R^2/Cond R^2		0.706/0.923		0.047/0.564	0.126/0.923		

* $p < 0.05$ ** $p < 0.01$ *** $p < 0.001$.

In contrast, for the Brightness Index (BI_2), the fixed component alone accounted for a significant portion of the variance ($R^2m = 0.706$). Specifically, BI_2, which indicates bare soil, was significantly lower in mature forests, closed forests, low forests, and shrublands (CL 1–6) compared to savannas and grasslands with trees (CL 7–8).

$MCARI_{Sent}$ values, which indicate leaf chlorophyll content, were significantly lower in mature forests of foothills (CL 1), mature forests of plains (CL 2), and closed forests (CL 3) compared to savannas (CL 7) and grasslands with trees (CL 8; Figure 3). Finally, $NDWI_{Gao}$ values were significantly higher in mature forests on plains and in the low closed forest of *Neltuma flexuosa* (CL 2 and CL 5) (Figure 2).

3.2. Structural Alteration Index Results Across Forest Classes

The structure and composition varied across the sampled sites, with the most altered sites in the plains landscape (i.e., those with high *SAI* levels—CL8 and CL7) characterized by a low cover of *Aspidosperma quebracho-blanco* and *Neltuma flexuosa* (Figure S3.1). These sites also exhibited a simplified vertical structure, low litter dry weight, lower seedling density of woody species, and cover and basal area of *Celtis ehrenbergiana*, high percentages of bare soil and high cover of *N. flexuosa* in the low woody layer, and of *Geoffroea decorticans* in all layers. In contrast, the most preserved sites (i.e., those with low *SAI* levels) on plains landscape (mature forests of CL 2) and partially also those of the foothills (mature forests of CL 1) exhibited opposite values for these structural variables. Sites with intermediate structural alteration (i.e., those with medium *SAI* levels), mainly referable to low closed forest (CL 5) and shrublands (CL 6), were characterized by high cover of *A. quebracho-blanco* in the low woody layer, *Larrea divaricata* in the lower and middle woody layers, and *Parkinsonia praecox* in all layers as well. These sites also showed high horizontal heterogeneity and tree density (S2, Figures S2.1 and S2.2). Furthermore, the most altered sites in the foothills, such as grasslands with trees (CL8) and savannas (CL7) (i.e., with high *SAI* levels), showed low

cover of *A. quebracho-blanco* and *N. flexuosa* in the high woody layer, as well as low vertical heterogeneity, litter dry weight, and seedling density of woody species. These sites had high percentages of bare soil and cover of *G. decorticans* and *L. divaricata* in the low woody layer, intermediate *N. flexuosa* cover in the low and middle woody layers, and moderate P. praecox cover in all layers. Conversely, the sites with low *SAI* referable to mature forests (CL1, CL2) and close forests (CL 3 and CL4) recorded opposite values for these variables. In contrast, the sites with intermediate *SAI* levels (mainly the low closed forest of CL 5 and shrublands CL 6) showed high *N. flexuosa* cover in the lower and middle layers, and *P. praecox* cover in all layers (S2, Figures S2.3 and S2.4).

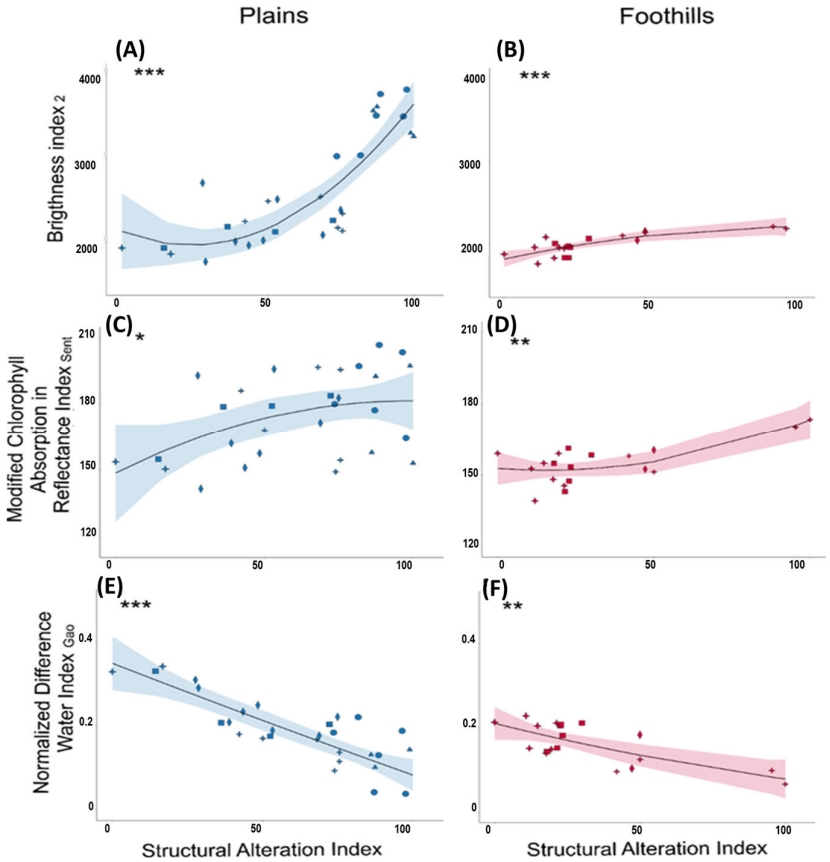

Figure 3. Relationship between spectral indices (annual average of BI_2, $MCARI_{Sent}$, $NDWI_{Gao}$) and *SAI* across forests on plains (blue, left) and foothills (red, right). Symbols indicate forest types: stars (mature forests, CL1-CL2), squares (closed forests with emergent, CL3-CL4), rhombuses (low closed forests, CL5), crosses (shrublands, CL6), triangles (savannas, CL7), circles (grasslands with trees, CL8). The black line represents the fitted model, with blue and red shading for the 95% confidence interval. Asterisks denote significance: * $p < 0.05$, ** $p < 0.01$, *** $p < 0.001$. Subfigures report: BI_2, relation with *SAI* values on plains (A), and foothills (B); $MCARI_{Sent}$, relation with *SAI* values on plains (C), and foothills (D); $NDWI_{Gao}$ relation with *SAI* values on plains (D), and foothills (E).

3.3. Relationship Between RS Variables and Field-Measured SAI Values

The relationship between RS spectral indices (annual averages of BI_2, $MCARI_{Sent}$, and $NDWI_{Gao}$) and *SAI* varied across forests in both the plains and foothills landscapes. Mean annual BI_2 showed a significant response to *SAI* across sites in both landscapes. Overall, mean annual BI_2 values increased at higher *SAI* levels in both landscapes (Figure 3A,B; Table 5). However, values recorded in foothills sites were 25% lower than those in the plains. Specifically, in the plains landscape, sites with *SAI* > 80% had significantly higher mean annual BI_2 values compared to sites with *SAI* < 80% (Adj $R^2 = 0.71$, $p < 0.0001$; Figure 3A). Both mean monthly and annual BI_2 values exhibited the same response pattern, with a

good overall fit (Adj $R^2 > 0.65$, $p < 0.0001$; S3, Figure S3.1; Table S3.1). In the foothills landscape, mean annual BI_2 also increased with *SAI* (Adj $R^2 = 0.54$, $p = 0.0002$; Figure 3B). Similarly, mean monthly BI_2 responded significantly to *SAI* for all months except November (Figure S3.1). The fit of mean monthly BI_2 values for the foothills sites was lower than that for the plains, ranging from Adj $R^2 = 0.14$ to 0.65 (S3, Table S3.1).

The mean annual $MCARI_{Sent}$ values of sites in both landscapes increased with greater *SAI* levels (S3, Figure S3.1; Table S3.1). However, 60% of the sites in the plains landscape fell outside the 95% confidence interval (Adj $R^2 = 0.15$, $p = 0.0185$; Figure 3C). The response of the mean monthly $MCARI_{Sent}$ to *SAI* varied across seasons. From February to May, $MCARI_{Sent}$ increased with higher *SAI* levels (S3, Figure S3.1). From December to January, $MCARI_{Sent}$ values showed no significant variation with *SAI* (S3, Figure S3.1; Table S3.1). In contrast, from September to November, $MCARI_{Sent}$ values decreased as *SAI* increased (S3, Figure S3.1). In the foothills landscape, mean annual $MCARI_{Sent}$ values also increased with higher *SAI* levels. The GLM for this landscape showed greater explanatory power compared to the plains, with only 40% of sites falling outside the 95% confidence interval (Adj $R^2 = 0.39$, $p = 0.0070$; Figure 3D). Similar to the plains, the response of monthly $MCARI_{Sent}$ values to *SAI* varied across months. From January to August, $MCARI_{Sent}$ increased with higher *SAI* levels (S3, Figure S3.1). From September to December, $MCARI_{Sent}$ values remained constant at increasing SAI levels (S3, Table S3.1).

Mean annual values of $NDWI_{Gao}$ decreased with increasing *SAI* levels in both landscapes (Figure 3E,F). In the plains landscape, sites with high *SAI* levels recorded significantly lower $NDWI_{Gao}$ values (Adj $R^2 = 0.71$, $p < 0.0001$; Figure 3E). This trend was consistent across monthly GLMs (S3, Figure S3.1), except for September, where $NDWI_{Gao}$ did not vary with *SAI* (S3, Table S3.1). In the foothills landscape, $NDWI_{Gao}$ values also declined with increasing SAI levels (Adj $R^2 = 0.52$, $p = 0.0003$; Figure 3F). From January to April, mean monthly $NDWI_{Gao}$ values remained relatively constant despite increasing *SAI* levels (S3, Figure S3.1, Table S3.1). However, from May to December, mean monthly $NDWI_{Gao}$ values mirrored the annual trend, decreasing with higher *SAI* levels (S3, Figure S3.1).

Table 5. Linear regressions between the Structural Alteration Index (*SAI*—predictor) and the spectral indices (BI_2, $MCARI_{Sent}$, and $NDWI_{Gao}$—response variables) for plain and foothill landscapes. The columns include landscape type; spectral index used as the response variable; adjusted Adj R^2 (model fit); sigma (residual error); F-statistic and its *p*-value (model significance); log likelihood and Akaike Information Criterion (AIC) for model evaluation; AIC of the null model (baseline comparison); number of observations (nobs); and *p*-value from the Shapiro–Wilk test assessing residual normality.

Landscape	RS ind	R^2 adj	Sigma	Statistic	*p*	logLik	AIC	AIC Null	Nobs	*p*-Value Shapiro-Wilk
Plains	BI_2	0.71	349.35	36.99	1.80×10^{-8}	−216.6	441.341	483	30	0.97
	$MCARI_{Sent}$	0.15	17.75	6.25	0.018	−127.8	261.679	265	30	0.16
	$NDWI_{Gao}$	0.71	0.047	73.58	2.50×10^{-9}	50.04	−94.083	−57	30	0.38
Foothills	BI_2	0.54	87.4	22.25	0.0002	−110.8	227.68	241	19	0.43
	$MCARI_{Sent}$	0.39	6.66	6.87	0.01	−61.35	130.7	138	19	0.36
	$NDWI_{Gao}$	0.52	0.03	20.15	0.00032	38.52	−71.04	−58	19	0.19

4. Discussion

Our findings highlight the substantial potential of spectral indices derived from Sentinel-2 imagery for assessing forest characteristics. The analysis of remote sensing ecological variables in the Arid Chaco region, encompassing both plains and foothills landscapes, effectively captures differences in forest conservation status associated with distinct management regimes. These differences, identified through field data (e.g., *SAI*) and corroborated by existing literature, further support the effectiveness of integrating remote sensing and field-based approaches for ecosystem assessment.

4.1. RS Variables Across Sampled Sites

The set of remote sensing variables selected through Variance Inflation Factor (VIF) analysis serves as reliable surrogates for key ecological aspects in subtropical semi-arid ecosystems. The Brightness Index (BI_2), a strong proxy for bare soil (Escafadal), can indicate varying levels of forest cover and degradation [83]. The Modified Chlorophyll Absorption in Reflectance Index ($MCARI_{Sent}$; [84]), which reflects leaf chlorophyll content, may help distinguish herbaceous vegetation—characterized by short-term productivity peaks during the vegetative period—from woody vegetation, which retains its leaves for longer periods [85,86]. The Normalized Difference Water Index ($NDWI_{Gao}$; Gao), an indicator of leaf water content, can capture the seasonal behavior of species with different drought adaptations [37,40]. The effectiveness of each ecological spectral index (BI_2, $MCARI_{Sent}$, and $NDWI_{Gao}$) in differentiating various forest conservation and management categories in the Arid Chaco region varies across temporal periods and months (Figure 4).

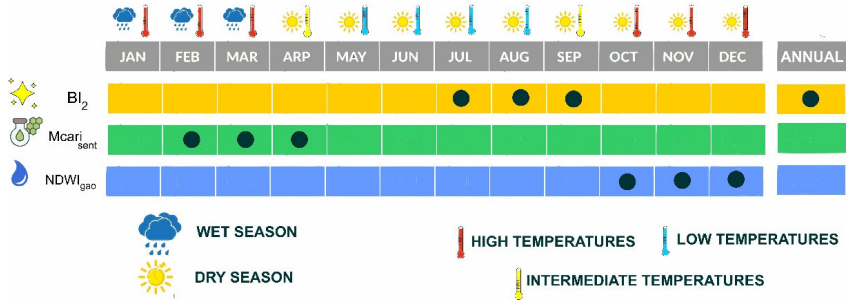

Figure 4. Temporal variability in the effectiveness of spectral indices (BI_2, $MCARI_{Sent}$, $NDWI_{Gao}$) in differentiating conservation and management categories of forests in the Arid Chaco. Wet (<70 mm) and dry (>70 mm) months, along with temperature levels (high: >25 °C, intermediate: 15–25 °C, low: <15 °C), are reported to capture seasonal forest dynamics.

Our results underscore the effectiveness of the Brightness Index (BI_2) in capturing vegetation phenology differences among forest classes with varying levels of resource utilization and extraction. In particular, BI_2 proved highly effective in differentiating savannas (CL 7) and grasslands with trees (CL 8), primarily used for intensified livestock raising, from formations with greater woody cover. Open formations, almost exclusively used for pastoral activities, exhibited significantly higher BI_2 values throughout the year, reflecting the prominence of bare soil surfaces. In contrast, natural formations with higher woody plant cover, such as mature forests on foothills and plains (CL 1–2), high forests (CL 3–4), and low forests and scrublands, all managed for multifunctional purposes such as timber extraction, grazing, aromatic herb collection, natural medicine production, and nature-based tourism [46], displayed significantly lower BI_2 values. These findings align with previous research conducted in the Chaco region and other semi-arid areas [37,83,87,88].

Although the application of the BI_2 index may have limitations in densely vegetated areas with closed canopies due to reduced bare soil visibility [37], it remains a valuable tool for monitoring dry forest lands, which cover over 10% of the world's forest area [89]. Despite these challenges, integrating the Brightness Index (BI_2) with other remote sensing variables has proven to be a reliable approach for distinguishing vegetation formations with different structures and levels of use in arid and semi-arid regions. Indeed, areas with high BI_2 values correspond to forests that have undergone significant modifications in structure and species composition. This observation is corroborated by the Structural Alteration Index (*SAI*) calculated for the analyzed sites, particularly in areas subjected to intensive livestock use (e.g., CL 6–8, Table 1).

The Modified Chlorophyll Absorption in Reflectance Index ($MCARI_{Sent}$), which reflects leaf chlorophyll content, effectively differentiates vegetation formations with varying

management regimes and conservation statuses (CL in Table 1). $MCARI_{Sent}$ values were significantly higher in savannas (CL 7) and grasslands with trees (CL 8), which are characterized by leaf renewal and productivity peaks during the summer. This is linked to vegetative growth during the subtropical rainy season, which triggers a rapid response in herbaceous species-dominated ecosystems, such as savannas and grasslands in subtropical regions worldwide [90]. In contrast, mature forest formations in plains and foothills (CL 1 and CL 2), dominated by woody species adapted to drought conditions (e.g., small leaves with thick cuticles and low photosynthetic rates to reduce transpiration), exhibited lower $MCARI_{Sent}$ values, consistent with previous studies in high-water-stress areas [91–93].

The observed pattern highlights a clear ecological distinction between mature forest formations on plains and foothill landscapes (e.g., CL 1 and 2), dominated by evergreen tree species adapted to water stress, such as *Aspidosperma quebracho-blanco* (drought-resistant; [94]), and deciduous species with deep root systems like *Neltuma flexuosa* (phreatophytic; [95]). In contrast, savannas and grasslands (e.g., CL 7 and 8), characterized by high grass and annual species cover, are more sensitive to variations in rainfall [96]. These findings demonstrate that significant ecological variations and management regimes within Chaco forests can be effectively detected through remote sensing, supporting the classification of analyzed landscapes into two primary groups: areas preserving natural forests for multifunctional management (e.g., within protected areas) and areas predominantly used for livestock grazing. Although this index exhibits weaker performance on an annual scale, certain months showed strong alignment across both landscape types, suggesting its potential as complementary information to the annual BI_2. This synergy enhances the ability of remote sensing ecological indices to distinguish different forest classes, thereby reinforcing structural discrimination capabilities. Previous studies have emphasized the value of using multiple remote sensing indices to improve accuracy in ecosystem characterization [97,98], underscoring the relevance of our results and their contribution to understanding structural dynamics in arid forests.

The Normalized Difference Water Index ($NDWI_{Gao}$), a key indicator of leaf water content, effectively distinguishes forest classes in the Arid Chaco. Moreover, it proves valuable in identifying forest classes dominated by tree species with different adaptations to drought conditions. $NDWI_{Gao}$ reveals notably higher leaf water content in plains forests dominated by *N. flexuosa* (CL 2 and CL 5), which are phreatophytes with well-developed root systems capable of accessing deep groundwater. In contrast, lowland forests growing on weakly developed stony soils (CL 1 and CL 3), dominated by *A. quebracho-blanco*, which has a shallow root system, exhibit remarkably low leaf water content [91–93]. Some secondary formations, such as shrublands dominated by *L. divaricata* (CL 6), savannas (CL 7), and grasslands (CL 8), also display low leaf water content values. This low $NDWI_{Gao}$ rate is likely due to the dominance of species in these classes that are more susceptible to the drought conditions characteristic of the Arid Chaco [85,86].

4.2. RS Ecological Variables Relationship with Field Integrity Values

The relationship between remote sensing spectral indices (annual averages of BI_2, $MCARI_{Sent}$, and $NDWI_{Gao}$) and the structural alteration of forests (*SAI*) varied across sites in both plains and foothills landscapes. The Brightness Index (BI_2) and the Modified Chlorophyll Absorption in Reflectance Index ($MCARI_{Sent}$) tend to increase in highly altered sites (e.g., with high *SAI* values), while $NDWI_{Gao}$ exhibited the opposite trend (Figure 3).

The Brightness Index (BI_2) showed a significant response to an increasing Structural Alteration Index (*SAI*) in both annual averages (Figure 3A,B; Table 5) and monthly averages. The robustness of this response may stem from the sensitivity of both indices—one derived from remote sensing and the other from field data—to the presence and extent of bare soil.

In the Chaco region, bare soil tends to cover larger areas in sites with low woody cover and high levels of silvopastoral and agricultural intervention (i.e., high *SAI*) [69,99,100]. This mosaic of woody vegetation patches intermingled with bare soil is characteristic of many dry forests worldwide, including the Chaco. In these ecosystems, degradation is often associated with an expansion of bare soil areas, and in severely degraded conditions, the landscape becomes dominated by bare soil [89,101]. The observed behavior of BI_2 and field-measured *SAI* across sites with different management pressures and conservation statuses effectively represents the forests of the Arid Chaco as highly heterogeneous, with woody vegetation distributed in a mosaic interspersed with bare soil and/or gaps [50,102]. Increasing intervention in these ecosystems (e.g., to enhance forage biomass) [103] inevitably leads to a simplification of vegetation structure and an increase in bare soil. The higher average BI_2 and *SAI* values in some sites within the plains landscape may be attributed to specific land uses, including megathermal pastures and crops, which result in greater seasonal exposure of bare soil [50]. These results highlight the potential of BI_2 as a reliable remote sensing indicator for differentiating sites with distinct conservation statuses within the Arid Chaco, allowing for assessments based on both annual averages and monthly data (Figure 3A,B).

The relationship between the Modified Chlorophyll Absorption in Reflectance Index ($MCARI_{Sent}$, annual average) and the Structural Alteration Index (*SAI*) showed moderate to weak correlations across sampled sites (Figure 3C,D; Table 5), likely due to phenological differences between the forest classes considered. The $MCARI_{Sent}$ index, a proxy for leaf chlorophyll concentration and canopy density, increased with *SAI* values during the wettest months (February to May) but showed no significant relationship during the driest months (June to December). Sites dominated by herbaceous cover (e.g., savannas and grasslands with trees, CL 7–8) exhibited lower annual chlorophyll concentrations than woody communities (e.g., mature, closed forests where evergreen and deciduous species with diverse drought stress strategies coexist, CL 1–4). However, during periods of active growth (e.g., humid summers and autumns), the simplified structure of grasslands and savannas and the minimal interference from non-photosynthetic elements (e.g., trunks and branches) allowed them to exhibit higher $MCARI_{Sent}$ values. Moreover, most crops and pastures receive supplemental irrigation from spring through early autumn [104].

Sites with high structural alteration values (*SAI* > 70%, CL 7–8), dominated by herbaceous species with shallow root systems highly dependent on monthly rainfall cycles, exhibited pronounced seasonal variability in $MCARI_{Sent}$ values [50,98,105]. This variability likely reflects the rapid physiological response of herbaceous species to rainfall, which triggers chlorophyll renewal and photosynthetic activity during wet periods [44,106]. In contrast, woody communities (CL 1–4) exhibited more stable $MCARI_{Sent}$ values due to their ability to access deeper water reserves through extensive root systems, decoupling their chlorophyll dynamics from surface rainfall patterns [91,107]. These contrasting strategies highlight the ecological mechanisms underlying seasonal differences in chlorophyll dynamics, with herbaceous vegetation relying on short-term water availability [108,109] and woody vegetation sustaining photosynthesis through long-term water reserves [106,110].

As a result, altered sites showed greater variability in biomass and chlorophyll content (e.g., $MCARI_{Sent}$ delta) between wet and dry seasons, with a clear relationship between $MCARI_{Sent}$ and *SAI* during wet periods (Figure 3C,D; Table 5). These results suggest that $MCARI_{Sent}$ is an effective indicator for monitoring ecosystems during wet periods, when vegetation reaches peak cover, productivity, and photosynthetic activity.

The Normalized Difference Water Index ($NDWI_{Gao}$), a proxy for vegetation water content, showed a significant inverse relationship with forest structural alteration (*SAI*) across sites. Beyond its ability to differentiate forests with varying alteration levels—an ability also demonstrated by BI_2 and $MCARI_{Sent}$—$NDWI_{Gao}$ enables more precise

differentiation of sites with high woody cover, particularly where the *SAI* is less than 30% (Figure 3E,F). High $NDWI_{Gao}$ values in well-preserved forests (*SAI* < 30%) effectively indicate the amount of biomass and water stored in the canopy, which is significantly greater compared to altered sites (*SAI* > 70%) [68]. $NDWI_{Gao}$ proved particularly effective in distinguishing forest classes with varying levels of *SAI* during periods of greatest water deficit. This seasonal behavior may be attributed to the ability of woody species to access deep water layers, allowing them to maintain stable foliar water levels during dry periods and decouple their water stress from seasonal rainfall [40,111]. Additionally, during this period, perennial herbaceous vegetation is dry (or in seasonal dormancy), and there is no cover of annual species, enabling a focus on structural differences in woody vegetation.

Previous studies have shown that species of the genus *Neltuma* exhibit remarkable adaptations for accessing deep groundwater reserves in arid and semi-arid regions. They employ a stratified root system with vertical roots extending to depths of 17 m to tap into groundwater, stabilizing growth during low-rainfall periods and mitigating water stress by relying on stable aquifers. This strategy is particularly relevant in environments such as the Arid Chaco, where surface water is scarce [112,113]. The ability of $NDWI_{Gao}$ to differentiate various woody communities' likely stems from the fact that those with adult individuals capable of accessing the water table can decouple their growth from the rainy season, unlike shallow-rooted species that rely solely on surface water. These findings highlight $NDWI_{Gao}$ as a valuable indicator for identifying well-preserved forest areas (i.e., low *SAI*) and an essential tool for monitoring forest ecosystem degradation in semi-arid regions such as the Arid Chaco.

Monitoring vegetation changes is particularly important in arid and semi-arid regions due to the sparse and sensitive nature of vegetation cover [114]. The correlation between remote sensing ecological indices (BI_2, $MCARI_{Sent}$, and $NDWI_{Gao}$) and field-measured forest structural alteration (*SAI*) suggests a strong potential for using these indices complementarily in forest monitoring in semi-arid landscapes. Seasonal monitoring is crucial in such ecosystems [114], and the phenological behavior of remote sensing ecological indices further strengthens their ability to distinguish different forest types throughout the year.

While BI_2 is applicable year-round, $NDWI_{Gao}$ and $MCARI_{Sent}$ exhibit seasonal sensitivity in detecting differences between communities dominated by various species and growth forms. These findings emphasize the value of integrating monthly remote sensing data to capture seasonal fluctuations in spectral indices, providing critical insights into vegetation responses to different management regimes.

5. Conclusions

Our findings highlight the significant potential of spectral indices derived from Sentinel-2 imagery for assessing forest characteristics and monitoring forest degradation in semi-arid landscapes such as the Arid Chaco. The Brightness Index (BI_2), Modified Chlorophyll Absorption in Reflectance Index ($MCARI_{Sent}$), and Normalized Difference Water Index ($NDWI_{Gao}$) proved effective in capturing differences in forest conservation status and structural alterations associated with varying management regimes and silvopastoral use.

BI_2 demonstrates robust year-round applicability, distinguishing open formations with high levels of bare soil from dense forests with greater woody cover. It is particularly effective in identifying sites with high structural alteration (e.g., intensive livestock use) due to its sensitivity to bare soil exposure. On the other hand, $MCARI_{Sent}$ excels during wet periods, reflecting seasonal variations in chlorophyll content and canopy density. It effectively differentiates sites with varying levels of structural alteration and highlights phenological differences among forest types, particularly in areas dominated by herbaceous species. $NDWI_{Gao}$ was especially useful in distinguishing forest types during dry periods, provid-

ing reliable insights into vegetation water content and differentiating forest types based on water-use strategies. Its sensitivity to leaf water content makes it particularly valuable for identifying well-conserved forest areas and vegetation adapted to drought conditions.

The seasonal variability of $MCARI_{Sent}$ and $NDWI_{Gao}$ complements the year-round applicability of BI_2, allowing for a nuanced understanding of vegetation structure, water stress adaptations, and conservation status. Together, these indices effectively differentiate sites with varying levels of forest degradation, reflecting differences in vegetation structure, water-use strategies, and management practices.

The integration of remote sensing (RS) indices with field-based measurements such as the Structural Alteration Index (*SAI*) further underscores the value of a hybrid approach for ecosystem monitoring. The strong correlations between RS indices and *SAI* values validate their utility as complementary tools for detecting and monitoring forest structural alteration and conservation status.

Monitoring vegetation changes is critical in all ecosystems, but particularly in arid and semi-arid regions, where vegetation cover is sparse and highly sensitive to environmental changes. Early detection of structural changes and assessment of their extent and severity at local and regional scales are therefore essential. In summary, the combined use of Sentinel-2 RS ecological variables (BI_2, $MCARI_{Sent}$, and $NDWI_{Gao}$) enhances our ability to monitor forest degradation, assess conservation efforts, and understand the ecological dynamics of semi-arid forests, making them valuable tools for sustainable land management and biodiversity conservation.

Despite the demonstrated effectiveness of these spectral indices, further efforts are needed to improve this phenology-based assessment. Incorporating Synthetic Aperture Radar (SAR) data or implementing spectral unmixing algorithms could enhance the accuracy and applicability of these analyses. Nevertheless, our results reveal distinct spectral differences between Arid Chaco forests under different management strategies, reinforcing the potential of RS-based approaches for ecosystem monitoring.

Our findings support the hypothesis that in highly seasonal subtropical forests, the phenological patterns of remote sensing ecological indices are influenced by ecosystem characteristics and the extent of alteration. This reinforces the crucial role of RS as a valuable proxy for modeling forest attributes. Incorporating a statistically sufficient number of field samples alongside monthly Sentinel-2 RS ecological indices would enhance the accuracy of large-scale assessments while significantly reducing costs compared to traditional field inventories.

From an applied perspective, the integration of field and RS data into a phenology-based forest conservation assessment provides relevant knowledge for forest monitoring and management. Considering that the data used are free and the procedures are standardized, the proposal could also be implemented by managing authorities to monitor the progress of the management models implemented. We encourage further studies to analyze increasingly larger areas to test the proposed approach and, at the same time, provide homogeneous information for forests in other biogeographical regions.

Supplementary Materials: The following supporting information can be downloaded at: https://www.mdpi.com/article/10.3390/rs17050748/s1, The supplementary material is organized into three main sections: S1, S2, and S3. Supplementary Material S1 includes Table S1.1, which details the Sentinel-2 imagery dataset, reporting the month, day, and hour of acquisition, the tiles, platform (Sentinel-2A or Sentinel-2B), and the cloud percentage. Table S1.2 provides a comprehensive list of all spectral indices derived from Sentinel-2 imagery, classified according to photosynthetic activity, water content, water stress, soil characteristics, chlorophyll content, and fire stress. Each index is described with its acronym, full name, required Sentinel-2 bands, and relevant bibliographic reference. Supplementary Material S2 includes Figure S2.1., which presents the Principal Component Analysis

(PCA) of sites based on field-measured structural and compositional variables of forests in the plains landscape, used to define the Structural Alteration Index. Figure S2.2. reports the contribution of variables to Principal Components 1 and 2 for sites sampled in the plains landscape. Figure S2.3. displays the Principal Component Analysis (PCA) of sites based on field-measured structural and compositional variables of forests in the foothills landscape, while Figure S2.4. reports the contribution of variables to Principal Components 1 and 2 for sites sampled in the foothills landscape. Table S2.1. Structure and composition variables derived from field sampling. Each index is described with its full name, acronym, formula and unit. Supplementary Material S3 presents the fitted models describing the relationship between remote sensing ecological indices (BI_2, $MCARI_{Sent}$ and $NDWI_{Gao}$) and the Structural Alteration Index across months in the plains and foothills landscapes. Figure S3.1. shows the fitted models and 95% confidence intervals for the monthly indices as a function of the Structural Alteration Index across forest types and landscapes. Table S3.1. reports the best-fitting monthly models for each spectral index and their relationship with the Structural Alteration Index (*SAI*) across forests in the plains and foothills landscapes. The table includes landscape type, the spectral index used as the response variable, adjusted R^2 (model fit), sigma (residual error), F-statistic and its *p*-value (model significance), log likelihood, and the Akaike Information Criterion (AIC) for model evaluation, as well as the AIC of the null model (baseline comparison). Additionally, the table provides the number of observations (*nobs*) and the *p*-value from the Shapiro–Wilk test assessing residual normality.

Author Contributions: Conceptualization, F.G.A., M.I., L.C., D.R.L. and M.L.C.; methodology, F.G.A., M.I., L.C., D.R.L., F.M. and M.L.C.; software, F.G.A., M.I. and R.R.-T.; validation, F.G.A., L.C. and D.R.L.; formal analysis, F.G.A., M.I., L.C., D.R.L. and M.L.C.; investigation, F.G.A., M.I., L.C., D.R.L., F.P., F.M., P.G., R.R.-T. and M.L.C.; resources, P.G. and M.L.C.; data curation, F.G.A., M.I., L.C. and R.R.-T.; writing—original draft preparation, F.G.A., M.I., L.C., D.R.L. and M.L.C.; writing—review and editing, F.G.A., M.I., L.C., D.R.L., F.P., F.M., P.G., R.R.-T. and M.L.C.; visualization, F.G.A., M.I. and L.C.; supervision, D.R.L., P.G. and M.L.C.; project administration, D.R.L., P.G. and M.L.C.; funding acquisition, P.G. and M.L.C. All authors have read and agreed to the published version of the manuscript.

Funding: This research was supported by the Great Relevance Italy and Argentina cooperation project ITAREO (ITalo-ARgentine Earth Observation technologies for the mapping of indicators for the United Nations Sustainable Development Goals—CUP: F15F21000620005); the Italian Recovery and Resilience Plan (National Biodiversity Future Centre—Urban Biodiversity; CUP H73C22000300001), the Italian Ministry for University and Research (D.M. n. 1062 del 10/08/2021—PON R&I 2014–2020, Research contracts on Green topics, CUP H55F21001490001, Code: 39-G-13537-2); and the PhD program on digital and environmental transition DM 118/2023 (M4C1–Inv. 3.4) CUP: H43C23000210001.

Data Availability Statement: The satellite images have been downloaded from the Copernicus Data Space Ecosystem. Other data may be available from the first author upon reasonable request.

Acknowledgments: We sincerely appreciate the European Space Agency for providing free satellite imagery, which has been instrumental in advancing our research. We are deeply grateful to the four reviewers and the editor for their constructive comments, which have greatly helped us improve the original version of the article.

Conflicts of Interest: The authors declare no conflicts of interest.

References

1. FAO. *State of the World's Forests 2022*; FAO: Rome, Italy, 2022.
2. Foley, J.A.; DeFries, R.; Asner, G.P.; Barford, C.; Bonan, G.; Carpenter, S.R.; Stuart Chapin, F.; Coe, M.T.; Daily, G.C.; Gibbs, H.K.; et al. Global Consequences of Land Use. *Science* **2005**, *309*, 570–574. [CrossRef] [PubMed]
3. Pacheco, P.; Mo, K.; Dudley, N.; Shapiro, A.; Aguilar-Amuchastegui, N.; Ling, P.Y.; Anderson, C.; Marx, A. *Deforestation Fronts: Drivers and Responses in a Changing World*; World's Wildlife Foundation: Gland, Switzerland, 2021.
4. Ghazoul, J.; Burivalova, Z.; Garcia-Ulloa, J.; King, L.A. Conceptualizing Forest Degradation. *Trends Ecol. Evol.* **2015**, *30*, 622–632. [CrossRef] [PubMed]

5. IPCC. *Good Practice Guidance for Land Use, Land-Use Change and Forestry*; Institute for Global Environmental Strategies for the IPCC: Geneva, Switzerland, 2003; ISBN 4887880030.
6. FAO. *Assessing Forest Degradation: Towards the Development of Globally Applicable Guidelines*; FAO: Rome, Italy, 2011.
7. Colglazier, W. Sustainable Development Agenda: 2030. *Science* **2015**, *349*, 1048–1050. [CrossRef]
8. Fassnacht, F.E.; White, J.C.; Wulder, M.A.; Næsset, E. Remote Sensing in Forestry: Current Challenges, Considerations and Directions. *Forestry* **2024**, *97*, 11–37. [CrossRef]
9. Carranza, M.L.; Hoyos, L.; Frate, L.; Acosta, A.T.R.; Cabido, M. Measuring Forest Fragmentation Using Multitemporal Forest Cover Maps: Forest Loss and Spatial Pattern Analysis in the Gran Chaco, Central Argentina. *Landsc. Urban Plan.* **2015**, *143*, 238–247. [CrossRef]
10. Gao, Y.; Skutsch, M.; Paneque-Gálvez, J.; Ghilardi, A. Remote Sensing of Forest Degradation: A Review. *Environ. Res. Lett.* **2020**, *15*, 103001. [CrossRef]
11. De Marzo, T.; Pflugmacher, D.; Baumann, M.; Lambin, E.F.; Gasparri, I.; Kuemmerle, T. Characterizing Forest Disturbances across the Argentine Dry Chaco Based on Landsat Time Series. *Int. J. Appl. Earth Obs. Geoinf.* **2021**, *98*, 102310. [CrossRef]
12. Schneibel, A.; Frantz, D.; Röder, A.; Stellmes, M.; Fischer, K.; Hill, J. Using Annual Landsat Time Series for the Detection of Dry Forest Degradation Processes in South-Central Angola. *Remote Sens.* **2017**, *9*, 905. [CrossRef]
13. Díaz-Delgado, R.; Lucas, R.; Hurford, C. *The Roles of Remote Sensing in Nature Conservation*; Springer: Cham, Switzerland, 2017; ISBN 978-3-319-64330-4.
14. Lloyd, D. A Phenological Classification of Terrestrial Vegetation Cover Using Shortwave Vegetation Index Imagery. *Int. J. Remote Sens.* **1990**, *11*, 2269–2279. [CrossRef]
15. Carranza, M.L.; Acosta, A.; Ricotta, C. Multitemporal Phenological Classification of Argentina. In *Analysis of Multi-Temporal Remote Sensing Images*; Buzzone, L., Smith, P., Eds.; World Scientific Publishing: Singapore, 2002; Volume 2, pp. 241–248.
16. Gray, R.E.J.; Ewers, R.M. Monitoring Forest Phenology in a Changing World. *Forests* **2021**, *12*, 297. [CrossRef]
17. Silveira, E.M.O.; Radeloff, V.C.; Martinuzzi, S.; Martinez Pastur, G.J.; Bono, J.; Politi, N.; Lizarraga, L.; Rivera, L.O.; Ciuffoli, L.; Rosas, Y.M.; et al. Nationwide Native Forest Structure Maps for Argentina Based on Forest Inventory Data, SAR Sentinel-1 and Vegetation Metrics from Sentinel-2 Imagery. *Remote Sens. Environ.* **2023**, *285*, 113391. [CrossRef]
18. De Marzo, T.; Gasparri, N.I.; Lambin, E.F.; Kuemmerle, T. Agents of Forest Disturbance in the Argentine Dry Chaco. *Remote Sens.* **2022**, *14*, 1758. [CrossRef]
19. Bucher, E.H. Chaco and Caatinga—South American Arid Savannas, Woodlands and Thickets. In *Ecology of Tropical Savannas*; Huntley, B.J., Walker, B.H., Eds.; Springer: Berlin, Germany, 1982; pp. 48–79.
20. Cabido, M.; Zeballos, S.R.; Zak, M.; Carranza, M.L.; Giorgis, M.A.; Cantero, J.J.; Acosta, A.T.R. Native Woody Vegetation in Central Argentina: Classification of Chaco and Espinal Forests. *Appl. Veg. Sci.* **2018**, *21*, 298–311. [CrossRef]
21. Adamoli, J.; Sennhauser, E.; Acero, J.M.; Rescia, A. Stress and Disturbance: Vegetation Dynamics in the Dry Chaco Region of Argentina. *J. Biogeogr.* **1990**, *17*, 491–500. [CrossRef]
22. Molina, S.I.; Valladares, G.R.; Gardner, S.; Cabido, M.R. The Effects of Logging and Grazing on the Insect Community Associated with a Semi-Arid Chaco Forest in Central Argentina. *J. Arid. Environ.* **1999**, *42*, 29–42. [CrossRef]
23. Rueda, C.V.; Baldi, G.; Gasparri, I.; Jobbágy, E.G. Charcoal Production in the Argentine Dry Chaco: Where, How and Who? *Energy Sustain. Dev.* **2015**, *27*, 46–53. [CrossRef]
24. Krapovickas, J.; Sacchi, L.V.; Hafner, R. Firewood Supply and Consumption in the Context of Agrarian Change: The Northern Argentine Chaco from 1990 to 2010. *Int. J. Commons* **2016**, *10*, 220–243. [CrossRef]
25. Cagnolo, L.; Cabido, M.; Valladares, G. Plant Species Richness in the Chaco Serrano Woodland from Central Argentina: Ecological Traits and Habitat Fragmentation Effects. *Biol. Conserv.* **2006**, *132*, 510–519. [CrossRef]
26. Macchi, L.; Grau, H.R.; Zelaya, P.V.; Marinaro, S. Trade-Offs between Land Use Intensity and Avian Biodiversity in the Dry Chaco of Argentina: A Tale of Two Gradients. *Agric. Ecosyst. Environ.* **2013**, *174*, 11–20. [CrossRef]
27. Mastrangelo, M.E.; Gavin, M.C. Impacts of Agricultural Intensification on Avian Richness at Multiple Scales in Dry Chaco Forests. *Biol. Conserv.* **2014**, *179*, 63–71. [CrossRef]
28. Torres, R.; Kuemmerle, T.; Zak, M.R. Changes in Agriculture-Biodiversity Trade-Offs in Relation to Landscape Context in the Argentine Chaco. *Landsc. Ecol.* **2021**, *36*, 703–719. [CrossRef]
29. Alvarez Arnesi, E.; López, D.R.; Barberis, I.M. Relationship between Degradation and the Structural-Functional Complexity of Subtropical Xerophytic Forests in the Argentine Wet Chaco. *Ecol. Manag.* **2024**, *562*, 121957. [CrossRef]
30. Frate, L.; Acosta, A.T.R.; Cabido, M.; Hoyos, L.; Carranza, M.L. Temporal Changes in Forest Contexts at Multiple Extents: Three Decades of Fragmentation in the Gran Chaco (1979–2010), Central Argentina. *PLoS ONE* **2015**, *10*, e0142855. [CrossRef]
31. Marchesini, V.A.; Fernández, R.J.; Reynolds, J.F.; Sobrino, J.A.; Di Bella, C.M. Changes in Evapotranspiration and Phenology as Consequences of Shrub Removal in Dry Forests of Central Argentina. *Ecohydrology* **2015**, *8*, 1304–1311. [CrossRef]
32. Giménez, R.; Mercau, J.; Nosetto, M.; Páez, R.; Jobbágy, E. The Ecohydrological Imprint of Deforestation in the Semiarid Chaco: Insights from the Last Forest Remnants of a Highly Cultivated Landscape. *Hydrol. Process* **2016**, *30*, 2603–2616. [CrossRef]

33. Magliano, P.; Fernández, R.; Gimenez, R.; Marchesini, V.; Páez, R.A.; Jobbágy, E. Changes in Water Fluxes Partition in the Arid Chaco Caused by the Replacement of Forest by Pastures. *Ecol. Austral* **2016**, *26*, 95–106. [CrossRef]
34. Boletta, P.E.; Ravelo, A.C.; Planchuelo, A.M.; Grilli, M. Assessing Deforestation in the Argentine Chaco. *Ecol. Manag.* **2006**, *228*, 108–114. [CrossRef]
35. Verón, S.R.; Blanco, L.J.; Texeira, M.A.; Irisarri, J.G.N.; Paruelo, J.M. Desertification and Ecosystem Services Supply: The Case of the Arid Chaco of South America. *J. Arid. Environ.* **2018**, *159*, 66–74. [CrossRef]
36. Abril, A.; Barttfeld, P.; Bucher, E.H. The Effect of Fire and Overgrazing Disturbes on Soil Carbon Balance in the Dry Chaco Forest. *Ecol. Manag.* **2005**, *206*, 399–405. [CrossRef]
37. Gasparri, N.I.; Grau, H.R. Deforestation and Fragmentation of Chaco Dry Forest in NW Argentina (1972–2007). *For. Ecol. Manag.* **2009**, *258*, 913–921. [CrossRef]
38. Baumann, M.; Gasparri, I.; Piquer-Rodríguez, M.; Gavier Pizarro, G.; Griffiths, P.; Hostert, P.; Kuemmerle, T. Carbon Emissions from Agricultural Expansion and Intensification in the Chaco. *Glob. Change Biol.* **2017**, *23*, 1902–1916. [CrossRef] [PubMed]
39. Barral, M.P.; Villarino, S.; Levers, C.; Baumann, M.; Kuemmerle, T.; Mastrangelo, M. Widespread and Major Losses in Multiple Ecosystem Services as a Result of Agricultural Expansion in the Argentine Chaco. *J. Appl. Ecol.* **2020**, *57*, 2485–2498. [CrossRef]
40. Steinaker, D.F.; Jobbágy, E.G.; Martini, J.P.; Arroyo, D.N.; Pacheco, J.L.; Marchesini, V.A. Vegetation Composition and Structure Changes Following Roller-Chopping Deforestation in Central Argentina Woodlands. *J. Arid. Environ.* **2016**, *133*, 19–24. [CrossRef]
41. Bigerna, M.; Bazylenko, A.; Torrella, S. Vegetation Phenology in the Argentinean Wet Chaco: Assessing Seasonality and Precipitation Dependence through NDVI—MODIS Time Series (2000–2018). *Austral Ecol.* **2022**, *47*, 629–640. [CrossRef]
42. Gasparri, N.I.; Baldi, G. Regional Patterns and Controls of Biomass in Semiarid Woodlands: Lessons from the Northern Argentina Dry Chaco. *Reg. Environ. Change* **2013**, *13*, 1131–1144. [CrossRef]
43. Blanco, L.J.; Paruelo, J.M.; Oesterheld, M.; Biurrun, F.N. Spatial and Temporal Patterns of Herbaceous Primary Production in Semi-arid Shrublands: A Remote Sensing Approach. *J. Veg. Sci.* **2016**, *27*, 716–727. [CrossRef]
44. Paruelo, J.M.; Texeira, M.; Staiano, L.; Mastrángelo, M.; Amdan, L.; Gallego, F. An Integrative Index of Ecosystem Services Provision Based on Remotely Sensed Data. *Ecol. Indic.* **2016**, *71*, 145–154. [CrossRef]
45. Barraza, V.; Grings, F.; Ferrazzoli, P.; Salvia, M.; Maas, M.; Rahmoune, R.; Vittucci, C.; Karszenbaum, H. Monitoring Vegetation Moisture Using Passive Microwave and Optical Indices in the Dry Chaco Forest, Argentina. *IEEE J. Sel. Top. Appl. Earth Obs. Remote Sens.* **2014**, *7*, 421–430. [CrossRef]
46. Cáceres, D.M. Accumulation by Dispossession and Socio-Environmental Conflicts Caused by the Expansion of Agribusiness in Argentina. *J. Agrar. Change* **2015**, *15*, 116–147. [CrossRef]
47. Zak, M.R.; Cabido, M.; Cáceres, D.; Díaz, S. What Drives Accelerated Land Cover Change in Central Argentina? Synergistic Consequences of Climatic, Socioeconomic, and Technological Factors. *Environ. Manag.* **2008**, *42*, 181–189. [CrossRef] [PubMed]
48. Torrella, S.A.; Ginzburg, R.G.; Adámoli, J.M.; Galetto, L. Changes in Forest Structure and Tree Recruitment in Argentinean Chaco: Effects of Fragment Size and Landscape Forest Cover. *Ecol. Manag.* **2013**, *307*, 147–154. [CrossRef]
49. Cabido, M.; Manzur, A.; Carranza, M.L.; Gonzalez Albarracin, C. La Vegetacion y El Medio Fisico Del Chaco Arido En La Provincia de Cordoba, Argentina Central. *Phytocoenologia* **1994**, *24*, 423–460. [CrossRef]
50. Alaggia, F.G. Integridad Ecológica En Paisajes Boscosos Bajo Uso Agropecuario: Configuración a Distintas Escalas Espaciales y Degradación En Bosques Del Chaco Árido. Ph.D. Thesis, Universidad de Buenos Aires, Buenos Aires, Argentina, 2024.
51. Zeballos, S.R.; Acosta, A.T.R.; Agüero, W.D.; Ahumada, R.J.; Almirón, M.G.; Argibay, D.S.; Arroyo, D.N.; Blanco, L.J.; Biurrun, F.N.; Cantero, J.J.; et al. Vegetation Types of the Arid Chaco in Central-Western Argentina. *Veg. Classif. Surv.* **2023**, *4*, 167–188. [CrossRef]
52. Morello, J.; Protomastro, J.; Sancholuz, L. Estudio Macroecologico de Los Llanos de La Rioja. In *Serie del Cincuentenario de la Administración de Parques Nacionales*; APN, Administración de Parques Nacionales, Secretariat de Agricultura, Ganadería y Pesca, Ministerio de Economía: Buenos Aires, Argentina, 1985.
53. Prado, D. What Is the Gran Chaco Vegetation in South America? I: A Review. Contribution to the Study of Flora and Vegetation of the Chaco. V. *Candollea* **1993**, *48*, 145–172.
54. Cabido, M.; González, C.; Acosta, A.; Díaz, S. Vegetation Changes along a Precipitation Gradient in Central Argentina. *Vegetatio* **1993**, *109*, 5–14. [CrossRef]
55. Carranza, C.A.; Ledesma, M. Bases Para El Manejo de Sistemas Silvopastoriles. In Proceedings of the XIII Congreso Forestal Mundial, Buenos Aires, Argentina, 18–25 October 2009.
56. Karlin, U.; Catalán, L.; Coirini, R.Y.; Zapata, R. *Uso y Manejo Sustentable de Los Bosques Nativos Del Chaco Arido*; Arturi, M.F., Frangi, J.L., Eds.; Ecología y Manejo de Bosques Nativos de Argentina, Universidad Nacional de La Plata: La Plata, Argentina, 2004.
57. Conti, G.; Enrico, L.; Jaureguiberry, P.; Cuchietti, A.; Lipoma, M.L.; Cabrol, D. The Role of Functional Diversity in the Provision of Multiple Ecosystem Services: An Empirical Analysis in the Dry Chaco of Córdoba, Central Argentina. *Ecosistemas* **2018**, *27*, 60–74. Available online: https://www.cabidigitallibrary.org/doi/full/10.5555/20203005848 (accessed on 18 December 2024).

58. Cavallero, L.; López, D.R.; Raffaele, E.; Aizen, M.A. Structural–Functional Approach to Identify Post-Disturbance Recovery Indicators in Forests from Northwestern Patagonia: A Tool to Prevent State Transitions. *Ecol. Indic.* **2015**, *52*, 85–95. [CrossRef]
59. Bestelmeyer, B.T.; Ash, A.; Brown, J.R.; Densambuu, B.; Fernández-Giménez, M.; Johanson, J.; Levi, M.; Lopez, D.; Peinetti, R.; Rumpff, L.; et al. State and Transition Models: Theory, Applications, and Challenges. In *Rangeland System*; Springer: Berlin/Heidelberg, Germany, 2017; pp. 303–345.
60. Drusch, M.; De Brito Ferreira, H.M.; Mandorlo, G. Sentinel-2 ESA's Optical High-Resolution Mission for GMES Operational Services STRV-1D. *Remote Sens. Environ ESA Commun.* **2012**, *120*, 25–36. [CrossRef]
61. Louis, J.; Pflug, B.; Main-Knorn, M.; Debaecker, V.; Mueller-Wilm, U.; Iannone, R.Q.; Giuseppe Cadau, E.; Boccia, V.; Gascon, F. Sentinel-2 Global Surface Reflectance Level-2a Product Generated with Sen2Cor. In Proceedings of the IGARSS 2019—2019 IEEE International Geoscience and Remote Sensing Symposium, Yokohama, Japan, 28 July–2 August 2019; IEEE: New York, NY, USA, 2019; pp. 8522–8525.
62. Barchuk, A.H.; Díaz, M.d.P. Vigor de Crecimiento y Supervivencia de Plantaciones de Aspidosperma Quebracho-Blanco y de Prosopis Chilensis En El Chaco Árido. *Quebracho Rev. Cienc. For.* **2000**, *8*, 17–29.
63. Alaggia, F.G.; Cabello, M.J.; Carranza, C.; Cavallero, L.; Daniele, G.; Erro Velazquez, M.; Ledesma, M.; Lopez, D.R.; Mussat, E.; Navall, J.M.; et al. *Manual de Indicadores para Monitoreo de Planes Prediales para el Manejo de Bosques con Ganadería Integrada (MBGI) Región Parque Chaqueño*; Agency of Access to Public Information: Buenos Aires, Agentina, 2019; ISBN 9789878697383.
64. Mueller-Dombois, D.; Ellenberg, H. *Aims and Methods of Vegetation Ecology*; John Willy & Sons: Hoboken, NJ, USA, 1974.
65. López-Martínez, J.O.; Sanaphre-Villanueva, L.; Dupuy, J.M.; Hernández-Stefanoni, J.L.; Meave, J.A.; Gallardo-Cruz, J.A. β-Diversity of Functional Groups of Woody Plants in a Tropical Dry Forest in Yucatan. *PLoS ONE* **2013**, *8*, e73660. [CrossRef] [PubMed]
66. Gareth, J.; Daniela, W.; Trevor, H.; Robert, T. *An Introduction to Statistical Learning: With Applications in R.*; Springer Science & Business Media: New York, NY, USA, 2017; ISBN 9781461471370.
67. Daughtry, C.S.T.; Walthall, C.L.; Kim, M.S.; De Colstoun, E.B.; McMurtrey, J.E. Estimating Corn Leaf Chlorophyll Concentration from Leaf and Canopy Reflectance. *Remote Sens. Environ.* **2000**, *74*, 229–239. [CrossRef]
68. Gao, B.-C. *NDWI—A Normalized Difference Water for Remote Sensing of Vegetation Water from Space*; Elsevier Science: Amsterdam, The Netherlands, 1996; Volume 7212.
69. Escadafal, R. Remote Sensing of Soil Color: Principles and Applications. *Remote Sens. Rev.* **1993**, *7*, 261–279. [CrossRef]
70. Nakagawa, S.; Schielzeth, H. A General and Simple Method for Obtaining R2 from Generalized Linear Mixed-effects Models. *Methods Ecol. Evol.* **2013**, *4*, 133–142. [CrossRef]
71. R Core Team. *R: A Language and Environment for Statistical Computing*; R Foundation for Statistical Computing: Vienna, Austria, 2023.
72. Wickham, H. *Ggplot2: Elegant Graphics for Data Analysis*; Springer: New York, NY, USA, 2016.
73. Bates, D.; Mächler, M.; Bolker, B.M.; Walker, S.C. Fitting Linear Mixed-Effects Models Using Lme4. *J. Stat. Softw.* **2015**, *67*, 1–48. [CrossRef]
74. Kassambara, A. *Package "rstatix" Title Pipe-Friendly Framework for Basic Statistical Tests*; Comprehensive R Archive Network: Vienna, Austria, 2023.
75. Hothorn, T.; Bretz, F.; Westfall, P. Simultaneous Inference in General Parametric Models. *Biom. J.* **2008**, *50*, 346–363. [CrossRef] [PubMed]
76. Lüdecke, D. *Package "sjPlot" Title Data Visualization for Statistics in Social Science*, R Package Version 2.8; R Foundation for Statistical Computing: Vienna, Austria, 2023.
77. Naimi, B.; Hamm, N.A.S.; Groen, T.A.; Skidmore, A.K.; Toxopeus, A.G. Where Is Positional Uncertainty a Problem for Species Distribution Modelling? *Ecography* **2014**, *37*, 191–203. [CrossRef]
78. Hernández-Stefanoni, J.L.; Gallardo-Cruz, J.A.; Meave, J.A.; Rocchini, D.; Bello-Pineda, J.; López-Martínez, J.O. Modeling (α- and β-Diversity in a Tropical Forest from Remotely Sensed and Spatial Data. *Int. J. Appl. Earth Obs. Geoinf.* **2012**, *19*, 359–368. [CrossRef]
79. Legendre, P.; Legendre, L. *Numerical Ecology*, 2nd ed.; Elsevier Science: Amsterdam, The Netherlands, 1998.
80. Zuur, A.F.; Ieno, E.N.; Walker, N.; Saveliev, A.A.; Smith, G.M. *Mixed Effects Models and Extensions in Ecology with R.*; Springer: New York, NY, USA, 2009; ISBN 978-0-387-87457-9.
81. Pebesma, E.; Bivand, R. *Spatial Data Science*, 1st ed.; Chapman and Hall/CRC: New York, NY, USA, 2023; ISBN 9780429459016.
82. Hijmans, R.J.; Bivand, R.; Pebesma, E.; Sumner, M.D. *Spatial Data Analysis*; Springer: Berlin/Heidelberg, Germany, 2024.
83. Huete, A.; Didan, K.; Miura, T.; Rodriguez, E.P.; Gao, X.; Ferreira, L.G. Overview of the Radiometric and Biophysical Performance of the MODIS Vegetation Indices. *Remote Sens. Environ.* **2002**, *83*, 195–213. [CrossRef]
84. Nagler, P.L.; Daughtry, C.S.T.; Goward, S.N. Plant Litter and Soil Reflectance. *Remote Sens. Environ.* **2000**, *71*, 207–215. [CrossRef]
85. Karlin, M.S.; Karlin, U.O.; Coirini, R.O.; Reati, G.J.; Zapata, R.M. *El Chaco Árido*; Editorial de la Universidad de Córdoba: Córdoba, Argentina, 2013.

86. Cabrera, H.M. *Fisiología Ecológica En Plantas: Mecanismos y Respuestas a Estrés En Los Ecosistemas*; Ediciones Universitarias de Valparaíso: Valparaíso, Chile, 2004.
87. Asner, G.P.; Elmore, A.J.; Olander, L.P.; Martin, R.E.; Harris, A.T. Grazing System, Ecosystem Response, and Global Change. *Annu. Rev. Environ. Resour.* **2004**, *29*, 261–299. [CrossRef]
88. Volante, J.N.; Alcaraz-Segura, D.; Mosciaro, M.J.; Viglizzo, E.F.; Paruelo, J.M. Ecosystem Functional Changes Associated with Land Clearing in NW Argentina. *Agric. Ecosyst. Environ.* **2012**, *154*, 12–22. [CrossRef]
89. Malagnoux, M. Afforestation and Sustainable Forests as a Means to Combat Desertification Arid Land Forests of the World Global Environmental Perspectives. In Proceedings of the Afforestation and Sustainable Forests as a Means to Combat Desertification, Jerusalem, Israel, 16–19 April 2007.
90. Walter, H.; Breckle, S.W. *Ecological Systems of the Geobiosphere: Tropical and Subtropical Zonobiomes*; Springer Science & Buisiness Media: Berlin/Heidelberg, Germany, 2013; Volume 2.
91. Jobbágy, E.G.; Sala, O.E.; Paruelo, J.M. Patterns and Controls of Primary Production in the Patagonian Steppe: A Remote Sensing Approach. *Ecology* **2002**, *83*, 307–319. [CrossRef]
92. Villagra, P.E.; Giordano, C.; Alvarez, J.A.; Cavagnaro, J.B.; Guevara, A.; Sartor, C.; Passera, C.B.; Greco, S. To Be a Plant in the Desert: Water Use Strategies and Water Stress Resistance in the Central Monte Desert from Argentina. *Ecol. Austral* **2011**, *21*, 29–42.
93. Moglia, J.G.; López, C.R. Estrategia Adaptativa Del Leño Aspidosperma Quebracho Blanco. *Madera Bosques* **2016**, *7*, 13–25. [CrossRef]
94. Chen, Z.; Li, S.; Wan, X.; Liu, S. Strategies of Tree Species to Adapt to Drought from Leaf Stomatal Regulation and Stem Embolism Resistance to Root Properties. *Front. Plant Sci.* **2022**, *13*, 926535. [CrossRef] [PubMed]
95. Kühnhammer, K.; van Haren, J.; Kübert, A.; Bailey, K.; Dubbert, M.; Hu, J.; Ladd, S.N.; Meredith, L.K.; Werner, C.; Beyer, M. Deep Roots Mitigate Drought Impacts on Tropical Trees despite Limited Quantitative Contribution to Transpiration. *Sci. Total Environ.* **2023**, *893*, 164763. [CrossRef] [PubMed]
96. López, D.R.; Cavallero, L.; Willems, P.; Bestelmeyer, B.T.; Brizuela, M.A. Degradation Influences Equilibrium and Non-equilibrium Dynamics in Rangelands: Implications in Resilience and Stability. *Appl. Veg. Sci.* **2022**, *25*, e12670. [CrossRef]
97. Gitelson, A.A.; Kaufman, Y.J.; Stark, R.; Rundquist, D. Novel Algorithms for Remote Estimation of Vegetation Fraction. *Remote Sens. Environ.* **2002**, *80*, 76–87. [CrossRef]
98. Lu, S.; Lu, F.; You, W.; Wang, Z.; Liu, Y.; Omasa, K. A Robust Vegetation Index for Remotely Assessing Chlorophyll Content of Dorsiventral Leaves across Several Species in Different Seasons. *Plant Methods* **2018**, *14*, 15. [CrossRef]
99. Ramírez-Juidias, E.; Amaro-Mellado, J.-L.; Antón, D. Wavelet Analysis of a Sentinel-2 Time Series to Detect Land Use Changes in Agriculture in the Vega Alta of the Guadalquivir River: Cantillana Case Study (Seville). *Remote Sens.* **2023**, *15*, 5225. [CrossRef]
100. Vieira, A.S.; do Valle Junior, R.F.; Rodrigues, V.S.; da Silva Quinaia, T.L.; Mendes, R.G.; Valera, C.A.; Fernandes, L.F.S.; Pacheco, F.A.L. Estimating Water Erosion from the Brightness Index of Orbital Images: A Framework for the Prognosis of Degraded Pastures. *Sci. Total Environ.* **2021**, *776*, 146019. [CrossRef]
101. Araujo, H.F.P.; Canassa, N.F.; Machado, C.C.C.; Tabarelli, M. Human Disturbance Is the Major Driver of Vegetation Changes in the Caatinga Dry Forest Region. *Sci. Rep.* **2023**, *13*, 18440. [CrossRef]
102. Ferraina, A.; Baldi, G.; de Abelleyra, D.; Grosfeld, J.; Verón, S. An Insight into the Patterns and Controls of the Structure of South America n Chaco Woodlands. *Land Degrad. Dev.* **2022**, *33*, 723–738. [CrossRef]
103. Guzmán, L.; Díaz, R.F.; Ricarte, A. Estimación Del Índice de Cosecha y Cálculo de La Receptividad Caprina a Escala de Potrer. In Proceedings of the III Congreso Argentino de Producción Caprina, Catamarca, Argentina, 29 December 2021; Volume 23, pp. 1–59.
104. Riera, C.; Barrionuevo, N. The Difusion of Mechanized Irrigation in Córdoba (1997–2011). *Rev. De. Geogr.* **2015**, *18*, 115–137.
105. Brown, T.P.; Hoylman, Z.H.; Conrad, E.; Holden, Z.; Jencso, K.; Jolly, W.M. Decoupling between Soil Moisture and Biomass Drives Seasonal Variations in Live Fuel Moisture across Co-Occurring Plant Functional Types. *Fire Ecol.* **2022**, *18*, 14. [CrossRef]
106. Piñeiro, G.; Oesterheld, M.; Paruelo, J.M. Seasonal Variation in Aboveground Production and Radiation-Use Efficiency of Temperate Rangelands Estimated through Remote Sensing. *Ecosystems* **2006**, *9*, 357–373. [CrossRef]
107. Sala, O.E.; Parton, W.J.; Joyce, L.A.; Lauenroth, W.K. Primary Production of the Central Grassland Region of the United States. *Ecology* **1988**, *69*, 40–45. [CrossRef]
108. Oesterheld, M.; Sala, O.E.; McNaughton, S.J. Effect of Animal Husbandry on Herbivore-Carrying Capacity at a Regional Scale. *Nature* **1992**, *365*, 234–236. [CrossRef] [PubMed]
109. Sala, E.; Ballesteros, E.; Dendrinos, P.; Di Franco, A.; Ferretti, F.; Foley, D.; Fraschetti, S.; Friedlander, A.; Garrabou, J.; Güçlüsoy, H.; et al. The Structure of Mediterranean Rocky Reef Ecosystems across Environmental and Human Gradients, and Conservation Implications. *PLoS ONE* **2012**, *7*, e32742. [CrossRef]
110. Paruelo, J.M.; Piñeiro, G.; Baldi, G.; Baeza, S.; Lezama, F.; Altesor, A.; Oesterheld, M. Carbon Stocks and Fluxes in Rangelands of the Río de La Plata Basin. *Rangel. Ecol. Manag.* **2010**, *63*, 94–108. [CrossRef]

111. Guzmán, L.M.; Villagra, P.E.; Quiroga, R.E.; Pereyra, D.I.; Pelliza, M.E.; Ricarte, A.R.; Blanco, L.J. In Search of Sustainable Livestock Management in the Dry Chaco: Effect of Different Shrub-Removal Practices on Vegetation. *Rangel. J.* **2023**, *44*, 193–202. [CrossRef]
112. Giordano, C.V.; Guevara, A.; Boccalandro, H.E.; Sartor, C.; Villagra, P.E. Water Status, Drought Responses, and Growth of Prosopis Flexuosa Trees with Different Access to the Water Table in a Warm South American Desert. *Plant Ecol.* **2011**, *212*, 1123–1134. [CrossRef]
113. Guevara, A.; Pancotto, V.; Mastrantonio, L.; Giordano, C.V. Fine Roots of Prosopis Flexuosa Trees in the Field. Plant and Soil Variables That Control Their Growth and Depth Distribution. *Plant Ecol.* **2018**, *219*, 1399–1412. [CrossRef]
114. Almalki, R.; Khaki, M.; Saco, P.M.; Rodriguez, J.F. Monitoring and Mapping Vegetation Cover Changes in Arid and Semi-Arid Areas Using Remote Sensing Technology: A Review. *Remote Sens.* **2022**, *14*, 5143. [CrossRef]